

Deep Learning for Human Mobility: a Survey on Data and Models

MASSIMILIANO LUCA, Fondazione Bruno Kessler (FBK), Italy and Free University of Bolzano, Italy

GIANNI BARLACCHI*, Amazon Alexa, Germany

BRUNO LEPRI, Fondazione Bruno Kessler (FBK), Italy

LUCA PAPPALARDO, Institute of Information Science and Technologies, National Research Council (ISTI-CNR), Italy

The study of human mobility is crucial due to its impact on several aspects of our society, such as disease spreading, urban planning, well-being, pollution, and more. The proliferation of digital mobility data, such as phone records, GPS traces, and social media posts, combined with the outstanding predictive power of artificial intelligence, triggered the application of deep learning to human mobility. In particular, the literature is focusing on three tasks: next-location prediction, i.e., predicting an individual's future locations; crowd flow prediction, i.e., forecasting flows on a geographic region; and trajectory generation, i.e., generating realistic individual trajectories. Existing surveys focus on single tasks, data sources, mechanistic or traditional machine learning approaches, while a comprehensive description of deep learning solutions is missing. This survey provides: (i) basic notions on mobility and deep learning; (ii) a review of data sources and public datasets; (iii) a description of deep learning models and (iv) a discussion about relevant open challenges. Our survey is a guide to the leading deep learning solutions to next-location prediction, crowd flow prediction, and trajectory generation. At the same time, it helps deep learning scientists and practitioners understand the fundamental concepts and the open challenges of the study of human mobility.

CCS Concepts: • **Computing methodologies** → **Artificial intelligence**; **Machine learning**; • **Applied computing** → **Transportation**.

Additional Key Words and Phrases: Human Mobility, Deep Learning, Datasets, Next-location Prediction, Crowd Flow Prediction, Trajectory Generation, Trajectory, Mobility Flows, Artificial Intelligence

ACM Reference Format:

Massimiliano Luca, Gianni Barlacchi, Bruno Lepri, and Luca Pappalardo. 2020. Deep Learning for Human Mobility: a Survey on Data and Models. 1, 1 (December 2020), 35 pages. <https://doi.org/10.1145/nnnnnnn.nnnnnnn>

*Work done before joining Amazon.

Authors' addresses: Massimiliano Luca, Fondazione Bruno Kessler (FBK), Via Sommarive, 19, Povo - Trento, Italy, Free University of Bolzano, Piazza Domenicani, 3, Bolzano, Italy, mluca@fbk.eu; Gianni Barlacchi, Amazon Alexa, , Berlin, Germany, gianni.barlacchi@gmail.com; Bruno Lepri, Fondazione Bruno Kessler (FBK), Via Sommarive, 19, Povo - Trento, Italy, ; Luca Pappalardo, Institute of Information Science and Technologies, National Research Council (ISTI-CNR), Via G. Moruzzi 1, 56124, Pisa, Italy, luca.pappalardo@isti.cnr.it.

2020. XXXX-XXXX/2020/12-ART \$15.00
<https://doi.org/10.1145/nnnnnnn.nnnnnnn>

1 INTRODUCTION

Urban population is increasing strikingly and human mobility is becoming more complex and bulky, affecting crucial aspects of people lives such as the spreading of viral diseases (e.g., the COVID-19 pandemics) [92, 95, 113, 116, 125, 138], the behavior of people in case of natural disasters [77, 156, 177], the public and private transportation and the resulting traffic volumes [27, 52, 86, 135], the well-being of citizens [122, 157, 173], the severity of air pollution, energy and water consumption [111, 159]. Furthermore, crowds' movement between cities is influenced by migrations from rural to urban areas, such as those induced by natural disasters, climate change, and conflicts [1, 65, 128, 132, 147].

Fortunately, policymakers are not unarmed in facing these challenges. The rise of ubiquitous computing (e.g., mobile phone, the Internet of Things, social media platforms) provides an always up-to-date and precise way to sense human movements at various temporal and spatial scales. Examples of mobility data include tracks from GPS devices embedded in smartphones [18, 96, 109, 127, 208], vehicles [11, 55, 118, 121] or boats [25, 51, 134, 184]; records produced by the communication between phones and the cellular network [16, 60]; and geotagged posts from social media platforms [15, 35, 82, 99, 129]. This deluge of digital data fostered a vast scientific production on various aspects of human mobility, such as the mining of trajectory data [78, 105, 174, 202, 206], the uncovering of the statistical patterns [6, 16, 60, 154], and the estimation of the privacy risk [37, 53, 123, 124, 126, 137]. The data availability also fostered a strand of literature on specific mobility tasks such as next-location prediction, crowd flow prediction, and trajectory generation.

Next-location prediction is the task of forecasting which location an individual will visit given historical data about their mobility. It is crucial in many applications such as travel recommendation, location-aware advertisements and geomarketing, early warning of potential public emergencies, and recommendation of friends in social network platforms [20, 179, 203, 204, 210]. Crowd flow prediction is the task of forecasting the incoming and outgoing flows of people on a geographic region, which has an impact on public safety, the definition of on-demand services, management of land use, and traffic optimization [44, 76, 145, 180, 195]. Trajectory generation is the task of generating synthetic trajectories that can reproduce, realistically, the individual and collective statistical patterns of human mobility [6, 70, 152, 175].

Although approaches based on Machine Learning (ML) achieve good results in solving these three tasks [20, 44, 145, 179, 180, 195, 204], the literature is now moving towards the design of Deep Learning (DL) solutions, motivated by the outstanding results obtained in computer vision, speech recognition, natural language processing and associated applications. DL solutions can deal more efficiently with heterogeneous and big data sources. On the one hand, they can extract relevant features from the data automatically [61], simplifying the combination of raw mobility data (e.g., trajectories, flows) and contextual information (e.g., weather data, traffic data, and census data). On the other hand, DL can capture complex and non-linear spatial, temporal, and sequential relationships in the data, thanks to a large number of parameters in Fully Connected (FCs), Convolutional (CNNs), and Recurrent Neural Networks (RNNs) [61].

For example, crowd flow predictors based on DL use several pipelines, based on CNNs and RNNs, to combine heterogeneous raw data (e.g., flows, graphs, weather conditions, events) and process the various spatio-temporal scales (e.g., short- and long-term temporal scales, near and far spatial regions) [2, 39, 80, 98, 100, 101, 131, 161, 166, 192, 197, 201, 211]. These pipelines allow extracting relevant features from the raw data automatically, a process that cannot be carried out with traditional ML approaches. Similarly, DL-based next-location predictors, exploiting CNNs and RNNs, can combine individual and collective mobility patterns and capture short and long temporal dependencies more effectively than traditional ML models [28, 36, 43, 47, 59, 90, 102, 104, 135, 185, 191]. Regarding trajectory generation, Generative Adversarial Networks (GANs) and autoencoders partially automate the generative model construction, capturing through CNNs and RNNs a wide set of spatio-temporal mobility

patterns automatically [48, 72, 94, 103, 115, 194]. This is an advantage over mechanistic generative models designed manually based on a limited set of well-known mobility patterns.

Given the advantages mentioned above, the literature on DL models for next-location prediction, crowd flow prediction, and trajectory generation is proliferating. Unfortunately, new approaches often do not benchmark against previous ones, mainly because they use different datasets, geographic setups, evaluation metrics. Existing surveys provide perspectives on single mobility tasks [6, 44, 70, 91, 145, 152, 180], focus on a single mobility data source [183, 204], or on traditional ML approaches [70, 175]. In this survey, we provide a comprehensive catalog of the DL solutions to all the three tasks and highlight for each of them the mobility and auxiliary datasets, geographical setups, evaluation metrics, and DL techniques used. In particular, we provide basic definitions of human mobility aspects, an introduction to fundamental concepts underlying DL techniques, characterization of peculiarities and limitations of the available mobility data sources, in companion with a list of public mobility and auxiliary datasets. We believe our survey can be beneficial to different profiles of scientists. On the one hand, our survey is a guide to DL concepts and mobility patterns, data sources, and tasks. On the other hand, it helps scientists and practitioners understand the leading DL solutions to next-location prediction, crowd flow prediction, and trajectory generation. In summary, this survey provides the reader with:

- An introduction to the concepts of trajectory, spatial tessellation, and mobility patterns (Sections 2.1, 2.2).
- An introduction to DL techniques and evaluation metrics of mobility tasks (Sections 2.3-2.7).
- A description of data sources such as mobile phone data (Section 3.1), GPS traces (Section 3.2), social media posts (Section 3.3), and other auxiliary data (Section 3.4); with a catalog of public datasets (Section 3).
- A definition of next-location prediction (Section 4.1), crowd flow prediction (Section 4.2) and trajectory generation (Section 4.3), with a discussion of the most relevant DL approaches' architectures, input data, and evaluation criteria.
- A discussion of the most interesting open challenges about the three tasks (Section 5).
- A GitHub repository (bit.ly/DL4HM) where researchers can co-operate to update the list of relevant mobility datasets and papers.

2 BACKGROUND

In this Section, we introduce useful concepts related to human mobility and deep learning. In Section 2.1, we define the concepts of trajectory and spatial tessellation. In Section 2.2, we describe human mobility patterns. In Sections 2.3-2.6, we discuss relevant deep learning techniques. Finally, in Section 2.7, we provide an overview of the metrics used in the literature to evaluate next-location and crowd flow predictors, and generative models.

2.1 Spatio-temporal trajectories and spatial aggregations

Mobility data describe the movements of a set of individuals during a period of observation. They are typically collected through electronic devices and stored in the form of spatio-temporal trajectories or mobility flows.

The *trajectory* of an individual is a sequence of records that allows for reconstructing their movements during the period of observation [206, 207]. Typically, each record contains the individual's identifier, a geographic location expressed as a spatial point, and a timestamp indicating when the individual stopped in or went through that location. Formally, we define a trajectory as follows:

Definition 2.1. Let u be an individual, a *trajectory* $T_u = \langle s_1, s_2, \dots, s_{n_u} \rangle$ is a time-ordered sequence composed by the n_u (semantic) spatio-temporal points visited by u . A spatio-temporal point is a pair $s = (t, l)$, where t indicates the time when point $l = (x, y)$ is visited by u , and x and y are spatial points in a given reference system (CRS), e.g., latitude and longitude. A semantic spatio-temporal point s is a tuple $s = (o, t, l)$, where t indicates the time when point $l = (x, y)$ is visited by u , l is a location expressed as coordinates (x, y) , and o is a parameter that brings some meaning to the point (e.g., home, workplace, or some other categories).

In some tasks, the geographic space is discretized by mapping the coordinates to a spatial *tessellation*, i.e., a covering of the bi-dimensional space using a countable number of geometric shapes called *tiles*, with no overlaps and no gaps. For instance, for crowd flow prediction tasks, a spatial tessellation is used to aggregate flows of people moving among locations (the tiles). Formally:

Definition 2.2. Given an area A , a set of geographical polygons called *tessellation*, \mathcal{G} , is defined with the following properties: (1) \mathcal{G} contains a finite number of polygons, l_i , called *tiles*, $\mathcal{G} = \{l_i : i = 1, \dots, n\}$; (2) the locations are non-overlapping, $l_i \cap l_j = \emptyset, \forall i \neq j$; (3) the union of all locations completely covers A , $\bigcup_{i=1}^n l_i = A$.

The tiling of the geographic space aims at creating the covering of the entire area of interest using regular tiles, such as equilateral triangular, squared, quadrilateral, or hexagonal tiles, or irregular tiles that may define the shape of buildings, census cells, or administrative units. A spatial join can be then used to associate each trajectory's point with the tile that contains it. Since the tessellation has no overlapping tiles and no gaps, each point is assigned to only one tile. Tessellations can be obtained exploiting open-source tools, such as scikit-mobility, S2 Geometry, and H3.¹ Figure 1 shows examples of tessellations in New York City.

S2 Geometry is an open-source project that represents spatial data on a three-dimensional sphere. It provides efficient and scalable spatial indexing techniques to carry out operations such as testing relationships among objects, measuring centroids, distances, and more. S2 Geometry decomposes the unit sphere into a hierarchy of cells (tiles), each of which is a quadrilateral bounded by four geodesics. The top level of the hierarchy is obtained by projecting the six faces of a cube into the unit sphere, and lower levels are obtained by subdividing each cell into four sub-cells recursively. Each cell in the hierarchy has a level, defined as the number of times the cell has been subdivided (starting with a face cell). Cells' levels range from 0 to 30. The smallest cells at level 30 are called leaf cells; there are 6×4^{30} cells in total, each about 1cm across on the Earth's surface.

The H3 geospatial indexing system consists of a hexagonal tiling of the sphere with hierarchical indexes. The hexagonal grid system is created on the planar faces of a sphere-circumscribed icosahedron, and the grid cells are then projected to the surface of the sphere using a specific projection. The H3 grid is constructed by recursively creating increasingly higher precision hexagon grids until the desired resolution is achieved. The first H3 resolution (resolution 0) consists of 122 base cells, and each subsequent resolution is created splitting each cell into seven children recursively. H3 provides 15 finer grid resolutions in addition to resolution 0. The finest resolution, resolution 15, has cells with an area of less than $1m^2$.

2.2 Human Mobility Patterns

Human movements, far from being random, follows well-defined statistical patterns [6, 175]. In this section, we revise the most relevant spatial (Section 2.2.1) and temporal (Section 2.2.2) patterns of human mobility.

2.2.1 Spatial patterns.

Displacements. The distance between two consecutive locations visited by an individual is called jump length or displacement [19, 60]. The term location usually indicates a spatial point in which an individual spent a minimum amount of time reflecting human behavioral tendencies that motivate people to move between two places. Formally, a jump length $\Delta r = d(s_i, s_{i+1})$ is the distance between two spatio-temporal points s_i and s_{i+1} in a trajectory $T_u = \langle s_1, s_2, \dots, s_n \rangle$. A truncated power-law well approximates the empirical distribution $P(\Delta r)$ within a population of individuals, with the value of the exponent slightly varying based on the type of data and the spatial scale [19, 60].

¹scikit-mobility [120]: <https://bit.ly/scikitmobility>, S2 Geometry: <https://s2geometry.io/>, Uber H3: <https://eng.uber.com/h3/>

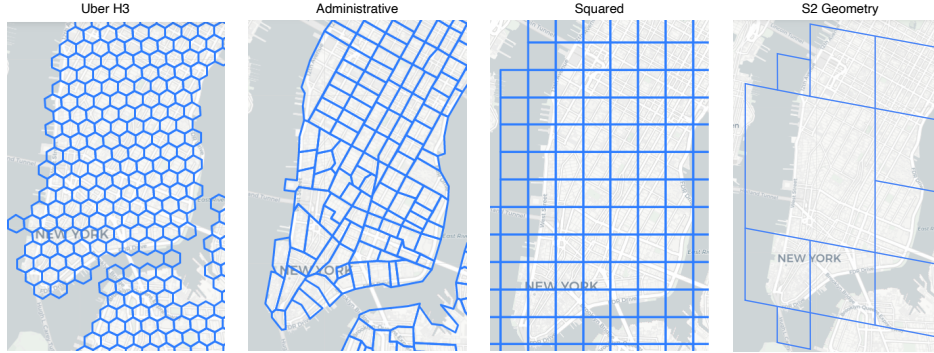


Fig. 1. Examples of spatial tessellations constructed over New York City. On the left, the city is tessellated in hexagons using H3 (resolution 6). In the second image, the area is split according to the administrative boundaries described in the GeoJSON file downloaded from New York City’s open data portal. In the third image, we use scikit-mobility to split an area into a squared grid with tiles of 1km×1km. In the last image, we make a tessellation using S2 Geometry.

Radius of gyration. The characteristic distance traveled by an individual u during a period of time can be quantified by their radius of gyration [60], defined as $r_g(u) = \sqrt{\frac{1}{n_u} \sum_{i=1}^{n_u} d(s_i, s_{cm})^2}$, where n_u is the number of points in T_u , $s_i \in T_u$ and $s_{cm} = \frac{1}{n_u} \sum_{i=1}^{n_u} s_i$ is the position vector of the center of mass of the set of points in T_u . A truncated power-law well approximates the distribution of r_g [60, 118]. At a collective level, the evolution in time of the average r_g of individuals follows a logarithmic curve $\langle r_g(t) \rangle \sim \alpha + \beta \ln t$ [60, 153].

The k -radius of gyration of an individual u is defined as the radius over their k most frequented locations [121], $r_g^{(k)}(u) = \sqrt{\frac{1}{N_k} \sum_{i=1}^k n_i d(s_i - s_{cm}^{(k)})^2}$, where $s_i \in T_u$, N_k is the sum of the visits to u ’s k most frequented locations, and $s_{cm}^{(k)} = \frac{1}{N_k} \sum_{i=1}^k s_i$ is the center of mass computed on u ’s k most frequented locations. The comparison of r_g and $r_g^{(k)}$ over an entire population revealed the existence of a returners and explorers dichotomy [121].

Mobility entropy. The temporal-uncorrelated entropy of an individual u characterizes the predictability of their spatial movements, and it is defined as $S_{unc}(u) = -\sum_{i=1}^{n_u} p_u(i) \log_2 p_u(i)$, where n_u is the number of distinct locations visited by u and $p_u(i)$ is the probability that u visits location i [42, 154]. The real entropy of an individual u considers also the order in which the places were visited and the time spent at each location, and it is defined as $S(u) = -\sum_{T'_u \subset T_u} P(T'_u) \log_2 P(T'_u)$ [154], where $P(T'_u)$ is the probability of finding a particular time-ordered subsequence T'_u in the trajectory T_u . The distribution of both S_{unc} and S are peaked and in particular $P(S)$ peaks around $S \approx 0.8$, indicating that the real spatio-temporal uncertainty in a typical user’s whereabouts is $2^{0.8} = 1.74$, i.e., fewer than two locations [154].

I-rank and G-rank. Location ranks identify the importance of a location to an individual’s mobility: the most visited location (likely home or work) has rank 1, the second most visited location (e.g., school or local shop) has rank 2, and so on. The visitation frequency of locations $P(L)$, or I-rank, follows a Zipf law: the probability of finding an individual at a location of rank L is well approximated by $P(L) \sim 1/L$ [60, 118]. Similarly, the collective visitation frequency of a location $P(r)$, or G-rank, indicates the popularity of locations according to how people visit them on the geographic space [115, 119].

Semantic importance. For an individual's trajectory T_u , we define $p_{d_{total}}(r) = \frac{d_{total}(r)}{\sum_r d_{total}(r)}$, where $d_{total}(r)$ is the total stay duration in location r interpreted as r 's semantic importance [14, 115]. The semantic distance between two trajectories T_u and T_v is the distance between the distribution of the $p_{d_{total}}(r)$ for u and v .

Mean Distance Error. Given two equal-sized sets of trajectories $\mathcal{T} = \{T_1, \dots, T_N\}$ and $\hat{\mathcal{T}} = \{\hat{T}_1, \dots, \hat{T}_N\}$, the Mean Distance Error (MDE) between \mathcal{T} and $\hat{\mathcal{T}}$ is defined as $MDE = \frac{\sum_i d(T_i, \hat{T}_i)}{N}$, where d is the distance between two points [72].

Mobility networks. In an individual mobility network (IMN), nodes represent locations and directed edges represent an individual's trips between locations [133, 142]. The vast majority of individuals' trips can be described with a limited number of daily motifs which represent the underlying regularities in daily movements [142]. Individual trajectories may be aggregated to study the flows of individuals between locations at different spatio-temporal scales. Flows can typically be described by an Origin-Destination (OD) matrix, or mobility network, which has a specific structure and dynamics [148].

2.2.2 Temporal metrics.

Waiting time and circadian rhythm. The waiting time Δt is the elapsed time between two consecutive points in the mobility trajectory of an individual u , or equivalently as the time spent in a location: $\Delta t = t_i - t_{i-1}$. Empirically the distribution of waiting times is well approximated by a truncated power-law [153]. The movements of individuals are not distributed uniformly during the hours of the day but follow a circadian rhythm [85, 119]; people tend to be stationary during the night hours while prefer moving at specific times of the day, for example, to reach the workplace or return home.

Temporal location patterns. The temporal popularity $p(r, t)$ measures the visiting probability for a location r at any time t [115]. The staying patterns $p(r, d)$ measures the probability of visiting a location r for a duration d [115].

2.3 Recurrent Neural Networks

A fully connected neural network (FC) consists of a series of fully-connected layers. All the neurons in one layer are connected to the neurons in the next layer. An FC layer, therefore, is a function that, given an input $x \in \mathcal{R}^m$, map values in $\mathcal{R}^m \rightarrow \mathcal{R}^n$ where m and n are the number of neurons in two consecutive layers. FCs are universal approximators (i.e., can learn any representation function) [61] but they are not able to deal with sequential data.

Recurrent Neural Networks (RNNs) [139] can efficiently deal with sequential data such as time series, in which values are ordered by time, or sentences in natural language, in which the order of the words is crucial to shaping its meaning. An RNN consists of a sequence of gates $G = \{G_0, \dots, G_{n-1}\}$, each one producing an hidden state h_i based on the current input x_i and the output from the previous gate h_{i-1} (Figure 2). In Vanilla RNNs, a gate G_i is implemented by using a hyperbolic tangent function (tanh), which takes as input x_i and h_{i-1} and computes the current state h_i . RNNs suffer from the vanishing gradient problem [89] and cannot propagate information found at early steps, losing relevant information at the beginning of a sequence when it is time to analyze its end [89]. Long-Short Term Memory networks (LSTMs) [71] and Gated Recurrent Units (GRUs) [30] are two gate implementations that mitigate this problem (Figure 2).

In LSTMs, the cell state c_i carries the data through the network, while the internal gates remove useless information from the flow or add relevant knowledge to the cell state. There are three internal gates: forget, input, and output gate (Figure 2). The forget gate passes the information of the previous hidden state h_{i-1} and of the current input x_i to a sigmoid activation function which ranges in $[0, 1]$. The closer the sigmoid's output (f_i) is to 0, the less likely the information is to be considered relevant. The sigmoid's output f_i is then pointwise

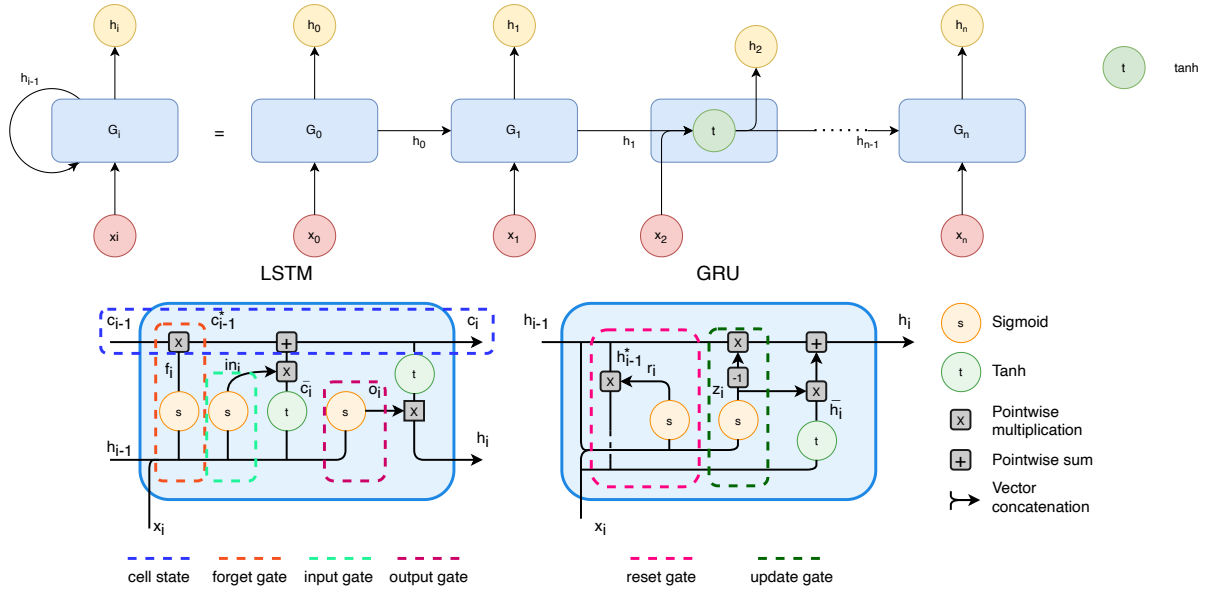


Fig. 2. (Top) An example of a Recurrent Neural Network (RNN). The right term of the equation corresponds to the unrolled version of the network on the left term. In general, an RNN takes as input a sequence $X = \langle x_0, x_1, \dots, x_n \rangle$ and produces an output h_i that, at a certain moment i , is based on the current input x_i and the output of the previous gate h_{i-1} . Usually, in Vanilla RNNs, the tanh function (green circle) is used to combine the current input x_i and the previous hidden state h_{i-1} . (Bottom) The structure of an LSTM gate (left) and a GRU gate (right). In the LSTM gate, we highlight with a dashed line the cell state (in blue), the forget gate (in orange), the input gate (in green), and the output gate (in purple). In the GRU gate, we highlight with the dashed line the reset gate (in red) and the update gate (in green).

multiplied with previous cell state c_{i-1} forming c_{i-1}^* . Values of c_{i-1}^* close to 0 are not taken into consideration by the current cell state. The input gate passes h_{i-1} and x_i to a sigmoid activation function and to a tanh activation function. The sigmoid function outputs in_i , i.e., the relevance of the new data (0 is not relevant; 1 is relevant). The tanh outputs, $\bar{c}_i \in [-1, 1]$, is multiplied with in_i , and the resulting product is pointwise summed with c_{i-1}^* to obtain the new cell state c_i . The output gate generates the hidden state h_i . The previous hidden state h_{i-1} and the current input x_i are passed to a sigmoid activation function, which generates o_i . This value is pointwise multiplied with the output of a tanh applied on the new cell state c_i , to form the new hidden state h_i . The hidden state h_i and the cell state c_i are passed to the next gate of the recurrent network. In some works, bidirectional LSTMs (Bi-LSTMs) [143] are adopted instead of LSTMs. Bi-LSTMs duplicate the recurrent layer: the sequence is provided as input to one layer and its reverse as input to the other layer. Analyzing time dependencies in both directions gives an advantage in scenarios like speech recognition, in which the context is essential to interpret the meaning of a sentence [63, 64].

In GRUs, the relevant information is propagated throughout the network using hidden states only (Figure 2). GRUs have two types of internal gates. The reset gate decides how much to forget and consists of a sigmoid function that takes as input the hidden layer of the previous step h_{i-1} and the current input x_i . The output of the sigmoid, r_i , is pairwise multiplied with h_{i-1} , generating h_{i-1}^* . Depending on h_{i-1}^* , we can determine which past information to forget (low values) or keep (high values). The update gate establishes whether the past information is relevant for future predictions and, therefore, should be propagated to the next steps. It is composed of a

sigmoid function that takes as input h_{i-1} and x_i and outputs z_i . The next hidden state, h_i , is obtained by: (i) computing \hat{h}_i , which is the output of a tanh function of h_{i-1}^* and the current input x_i ; (ii) multiplying $1 - z_i$ with h_{i-1} ; and (iii) adding the resulting sum to the product between z_i and \hat{h}_i .

RNNs are widely used in next-location prediction (Section 4.1), often in combination with attention mechanisms, to capture the temporal relationships in individual trajectories. Moreover, RNNs are often combined with convolutional neural networks in crowd flow prediction (Section 4.2) and trajectory generation (Section 4.3), to capture temporal and spatial patterns at the same time.

2.4 Convolutional Neural Networks

Convolutional Neural Networks (CNNs) are widely used in computer vision for their efficacy in object recognition [130, 149], image classification and segmentation [46, 93], movement or event recognition [170], and more [87]. Similarly to the visual cortex [74, 75], a CNN is a network made of neurons that react only to certain stimuli in a restricted region of the visual field [93].

CNNs alternate two types of layers: (i) the convolutional layers reduce the size of the matrix by applying a kernel function, or filter, that keeps all the relevant information; (ii) the pooling layers reduce the spatial size of the convoluted features to decrease the computational power required to process the data. Figure 3 shows an example of a CNN architecture with two convolutional layers and two pooling layers. Usually, at the end of the CNN, an FC is used to compute the output.

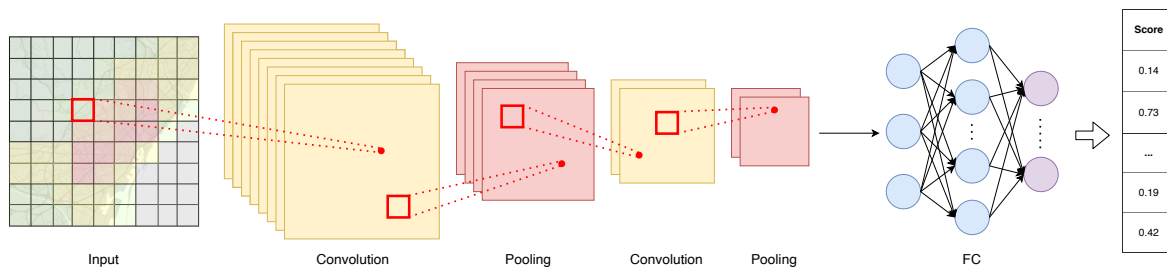


Fig. 3. Example of architecture of a CNN. The neural network consists of two convolutions and two pooling layers. After the convolution/pooling layers, there is an FC that outputs the prediction. For instance, to classify a sample into one of n classes, the last layer is usually fed into an FC that outputs a $1 \times n$ vector containing the probabilities of the sample to belong to a specific class.

The convolutional layers apply one or more filters to the input matrix A to extract relevant features and summarize the characteristics of an $i \times j$ area of A into a single value. Specifically, given an input matrix A of size $n \times m$, a filter is a mathematical operation between the original matrix A and another matrix B of size $k \times l$, with $k < n$ and $l < m$. The filter is generally applied with a sliding window mechanism called stride.

The pooling layers aim at downsampling the input matrix, replacing each portion of it with summary statistics. In practice, pooling layers are either max pooling or average pooling. Max pooling returns the maximum value from the part of the matrix convoluted by a given size and stride filter. Average pooling returns the average of the values produced by the filter operations. Pooling layers create representations of the matrix that are approximately invariant to small translations of the input.

A significant limitation of CNNs, especially relevant for networks with many layers, is the vanishing gradient issue [89]. The so-called residual units are a solution to this problem [69]. A residual unit implements the skip connection also known as identity connection. Given a network with l_1, \dots, l_k layers, the output of a layer l_i is

added to the output of the layer l_{i+j} so to preserve the loss of information. The variable j represents the skip size, and it is usually smaller than 4.

Differently from RNNs, where the input is processed sequentially, CNNs are not designed to process sequences, and they are used mainly in crowd flow prediction (Section 4.2): the evolution of the incoming (outgoing) flows within a city is represented as a sequence of matrices. CNNs are used to capture the dynamics of the spatial dependencies among the areas of a city. CNNs are often combined with RNNs to capture temporal dependencies (e.g., ConvLSTM [181]). CNNs are also used in trajectory generation (Section 4.3): real trajectories are represented as images and used to train a Generative Adversarial Network (GAN), in which two CNNs are used as generator and discriminator to generate realistic trajectories.

2.5 Attention Mechanism

Attention mechanisms are based on the idea that, when dealing with a large amount of information, our brains focus on the most significant parts and consider all the others as background information. Initially introduced for natural language processing (e.g., machine translation [31, 162] and speech recognition tasks [33]), the usage of attention mechanisms rapidly extended to computer vision, healthcare, and recommendation systems [32, 144, 182]. Given the current input x and a context, an attention mechanism produces a score for each element of x . These scores are usually computed using adequate activation functions (e.g., softmax) and organized in a vector s . A context vector \hat{c} is computed as the pairwise multiplication between s and x . The context plays a crucial role in the establishment of which features should be the most important to the model.

2.6 Generative Adversarial Networks

Generative adversarial networks (GANs) [62] are an example of generative models, i.e., any model that takes a training set, consisting of samples drawn from a distribution, and learns to represent an estimate of that distribution. A generative mobility model can generate synthetic spatio-temporal trajectories that realistically reproduce mobility patterns. Recently, GANs are being used to generate synthetic mobility trajectories [103, 115].

The basic idea of a GAN is to set up a game between a generator (e.g., a neural network) and a discriminator (e.g. a classifier) (Figure 4). The generator creates samples from the distribution p_g that are intended to come from the same distribution as the training data p_{data} and hence similar to the original ones. The discriminator examines the generated samples to determine whether they are real or fake. In other words, the generator is trained to fool the discriminator by generating samples that are indistinguishable from real ones.

Mathematically, the generator and the discriminator are two functions that are differentiable with respect to both the inputs and the parameters. The discriminator is a function D that takes x (e.g., a trajectory) as input and uses $\Theta^{(D)}$ as parameters. The generator is a function G that takes z (e.g., set of trajectories) as input and uses $\Theta^{(G)}$ as parameters. D wishes to minimize a cost function $J(D)(\Theta^{(D)}, \Theta^{(G)})$ while controlling only $\Theta^{(D)}$. Similarly, G wishes to minimize a cost function $J(G)(\Theta^{(D)}, \Theta^{(G)})$ while controlling only $\Theta^{(G)}$. This scenario is a game the solution of which is a Nash equilibrium [61], i.e., a tuple $(\Theta^{(D)}, \Theta^{(G)})$ that is a local minimum of $J(D)$ with respect to $\Theta^{(D)}$ and a local minimum of $J(G)$ with respect to $\Theta^{(G)}$.

The training process consists of two simultaneous Stochastic Gradient Descent (SGD) [61]. SGD is a stochastic approximation of gradient descent optimization that replaces the actual gradient with an estimate, thus achieving faster iterations in trade for a lower convergence rate. Two gradient steps are made simultaneously: one updating $\Theta^{(D)}$ to reduce $J(D)$ and one updating $\Theta^{(G)}$ to reduce $J(G)$. Usually, the cost function used for the discriminator and the generator is the cross-entropy [61], defined as: $H(P, Q) = -E_P[\log Q]$, where P, Q are two distributions and E_P is the expected value of $\log Q$ according to P .

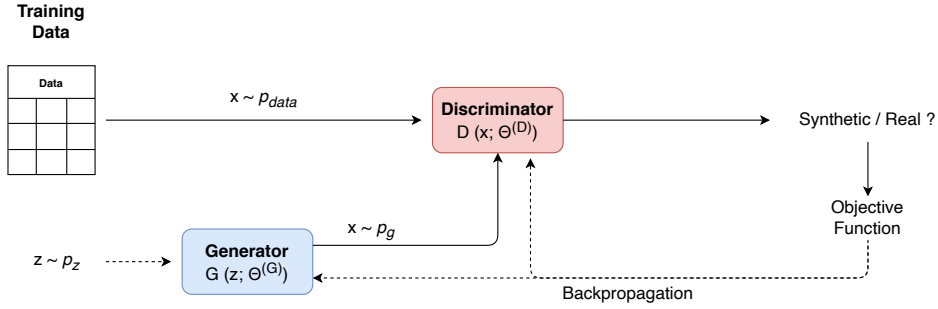


Fig. 4. Visual representation of a Generative Adversarial Network (GAN). A GAN is composed of a generator G , and a discriminator D . The generator is a differentiable function $G(z; \Theta^{(G)})$ which outputs the new data according to a distribution p_g , where $\Theta^{(G)}$ are the parameters of the generative model. The discriminator represents a differentiable function $D(x; \Theta^{(D)})$, where $\Theta^{(D)}$ are the parameters of the discriminative model, which produces the probability that x comes from the distribution of training data p_{data} . The aim is to obtain a generator that is a good estimator of p_{data} . When this occurs, the discriminator is "fooled" and can no longer distinguish the samples from p_{data} from those from p_g .

2.7 Evaluation Metrics

In the literature, the performance of predictive and generative models is evaluated using specific metrics. In this section, we describe the most common metrics used in the literature.

2.7.1 Error measures. Mean Absolute Error (MAE), Mean Squared Error (MSE), Root Mean Squared Error (RMSE), and Mean Absolute Percent Error (MAPE) measure the magnitude of the errors in a set of predictions:

$$\text{MAE} = \frac{1}{n} \sum_{i=1}^n |y_i - \hat{y}_i|; \quad \text{MSE} = \frac{1}{n} \sum_{i=1}^n (y_i - \hat{y}_i)^2; \quad \text{RMSE} = \sqrt{\frac{1}{n} \sum_{i=1}^n (y_i - \hat{y}_i)^2}; \quad \text{MAPE} = \left(\frac{1}{n} \sum_{i=1}^n \frac{|y_i - \hat{y}_i|}{|y_i|} \right) * 100 \quad (1)$$

where \hat{y}_i indicates the predicted value, y_i indicates the actual value, and n is the number of predictions. All metrics range in $[0, \infty]$ and lower values indicate better performance. Since MAE uses the error's absolute value, it does not consider whether the model overestimates or underestimates the actual value. On the other side, MSE weighs large errors more than MAE, and it is sensitive to outliers. RMSE weighs the errors more than MAE, hence penalizing models that produce large errors. As the values are squared, the RMSE is expressed in the same unit as the predicted one.

2.7.2 Distances. The *Haversine distance* is the distance on the spherical earth² between two points p_1 and p_2 :

$$d_h(p_1, p_2) = 2R \left(\sqrt{\frac{a(p_1, p_2)}{a(p_1, p_2) - 1}} \right); \quad a(p_1, p_2) = \sin^2 \left(\frac{\phi_2 - \phi_1}{2} \right) + \cos(\phi_1) \cos(\phi_2) \sin^2 \left(\frac{\lambda_2 - \lambda_1}{2} \right) \quad (2)$$

where R is the earth radius and λ_i and ϕ_i , with $i = 1, 2$, are the longitude and the latitude of p_i , respectively. The Haversine distance range in $[0, \infty]$ and lower values indicate better performance. Another way to compute the distance between two points p_1, p_2 is the *equirectangular distance*, defined as:

$$d_{eq}(p_1, p_2) = R \sqrt{\left((\lambda_{p_2} - \lambda_{p_1}) \cos \left(\frac{\phi_{p_2} - \phi_{p_1}}{2} \right) \right)^2 + (\phi_{p_2} - \phi_{p_1})^2} \quad (3)$$

²Flat earthers can simply use the Euclidean distance, defined as follows: given two points $p_1 = (x_1, y_1)$ and $p_2 = (x_2, y_2)$, $d_{\text{flaearth}} = \sqrt{(x_1 - x_2)^2 + (y_1 - y_2)^2}$

where λ_{p_i} and ϕ_{p_i} are the longitude and latitude of point p_i , respectively.

2.7.3 Accuracy and k -accuracy. In machine learning, Accuracy (ACC) is the ratio of correctly predicted observations. In next-location prediction, ACC indicates how many of the locations an individual will visit are correctly predicted by the model. However, the k -accuracy (ACC@ k) is often used instead of ACC: predictors output a list of all possible locations an individual can visit next, ranked from the most to the least likely; ACC@ k is the fraction of times the real location is among the k most likely locations predicted by the model, i.e., the percentage that a list of predictions with length k covers the ground truth location (ACC = ACC@1).

2.7.4 Precision, Recall, and F1-score. These metrics are used to evaluate the performance of next-location predictors. Precision measures how accurate the model is on the positive class. Recall measures the True Positive Rate (TPR), i.e., the fraction of positive instances correctly predicted by the model. F1-score summarizes the performance of a model and it is computed as the harmonic mean of Precision and Recall. Given the number of True Positives (TPs), False Positives (FPs), and False Negatives (FNs), we define Precision, Recall, and F1-Score as:

$$\text{Precision} = \frac{TP}{(TP + FP)}; \quad \text{Recall} = \frac{TP}{(TP + FN)}; \quad F1 = 2 \frac{\text{Precision} \times \text{Recall}}{\text{Precision} + \text{Recall}} \quad (4)$$

2.7.5 Area Under the Curve. The Receiver Operating Characteristic Curve (ROC) visualizes a classifier's performance by plotting the Recall against the False Positive Rate (FPR). FPR is the ratio of FPs over the sum of FPs and True Negatives (TNs). AUC ($\in [0, 1]$) measures the area under the ROC. It is scale-invariant and provides an aggregate measure of performance across all possible classification thresholds. The higher the AUC, the better the model, where AUC=0.50 indicates the performance of a model that makes predictions at random.

2.7.6 Divergence metrics. The Kullback-Leibler (KL) divergence measures how different a probability distribution is from a reference probability distribution. It is used to assess the performance of a generative mobility model by calculating the extent to which synthetic trajectories and real trajectories are similar with respect to relevant mobility patterns. Formally, given two discrete probability distributions P and Q , defined on the same probability space X , the KL divergence from P to Q is defined as:

$$D_{\text{KL}}(P||Q) = \sum_{x \in X} P(x) \log \left(\frac{P(x)}{Q(x)} \right). \quad (5)$$

Formally, given two probability distributions P and Q , KL divergence is the expectation of the logarithmic difference between the probabilities of P and Q , where the expectation is taken using the probabilities of P . KL divergence is always non-negative ($D_{\text{KL}}(P||Q) \geq 0$) and not symmetric, i.e., $D_{\text{KL}}(P||Q) \neq D_{\text{KL}}(Q||P)$. P and Q are the same distribution if $D_{\text{KL}}(P||Q) = 0$.

The Jensen-Shannon (JS) divergence is a measure to assess the similarity between two distributions. It is based on the KL divergence but it is symmetric ($JS(P||Q) = JS(Q||P)$) and ranges in $[0, 1]$. Formally, given two probability distributions P and Q , and $M = \frac{1}{2}(P||Q)$, we define the JS divergence as:

$$D_{\text{JS}}(P||Q) = \frac{1}{2}D_{\text{KL}}(P||M) + \frac{1}{2}D_{\text{KL}}(Q||M). \quad (6)$$

The JS divergence is used, as an alternative to KL, to assess the performance of generative mobility models.

3 HUMAN MOBILITY DATA

The last decade has witnessed the emergence of massive datasets of digital traces that portray human movements at an unprecedented scale and detail. Examples include tracks generated by GPS devices embedded in smartphones [208] or private vehicles [118]; mobile phone records [16]; and geotagged posts from social media platforms [110]. Unfortunately, most of these datasets are proprietary and not publicly available, making research on human

mobility hard to reproduce. In this section, we discuss the peculiarities of various sources of mobility data. For each data source, we provide a reference to a list of datasets that are available for research (Table 1). We identify and discuss three primary data sources: mobile phone data (Section 3.1), GPS traces (Section 3.2), and social media data (Section 3.3). Moreover, in Section 3.4 we discuss data sources that convey important auxiliary information (traffic, environmental, and census and administrative data).

3.1 Mobile Phone data

Nowadays, mobile phones are ubiquitous, with coverage in most countries that reaches almost 100% of the population [16, 171]. Telco companies record the activity of their users for billing and operational purposes, hence storing an enormous amount of information on where, when, and with whom users communicate [16].

Every time a user engages a telecommunication interaction – makes or receives a call or a text message, or uses the mobile data connection – the operator assigns a Radio Base Station (RBS) to deliver the communication through the network. Since the position and the coverage area of each RBS are known, a user’s telecommunication interaction reflects their geographic location. Each telecommunication interaction generates several mobile data formats, the most used of which are Call Detail Records (CDRs) and eXtended Detail Records (XDRs) [117].

Every time a user makes/receives a call or sends/receives an SMS, a new Call Detail Record (CDR) is created recording the time of the interaction, the RBSs that handled it, and the two users’ anonymized identifiers. A CDR is a tuple $(u_o, u_i, t, A_o, A_i, d)$, where u_o and u_i are the identifiers of the caller and the callee, respectively, and t is a timestamp of when the call starts. In turn, A_o and A_i are the RBSs that manage the outgoing call and the receiving call, respectively, and d is the call duration. An individual’s mobility can be reconstructed from CDRs assuming a movement between the RBSs of any two consecutive records [16]. Aggregated mobility, such as crowds’ movements, can be inferred by counting the number of users that move, in a given time window, between two RBSs or spatial aggregations of them (e.g., neighborhoods or municipalities) [21]. CDRs are sparse in time, i.e., a user’s position is known when they make or receive a call or a text message only, leading to sparse and incomplete mobility trajectories. Notwithstanding, CDRs are by far the most common format of mobile phone records, used for a large number of studies on human mobility [7, 16, 34, 60, 121, 148].

When a user uploads or downloads data from the Internet using their phone’s mobile connection, they generate an eXtended Detail Record (XDR), a tuple (u, t, A, k) where A is the RBS that serves the connection, and k the amount of uploaded/downloaded information. XDRs are less common in the literature than CDRs, mainly because the advent of the mobile data connection is relatively recent. XDRs partially overcome the problem of sparsity present in CDRs [26], because mobile connections are more frequent than calls and text messages.

For both CDRs and XDRs, the spatial granularity is at the level of RBS, i.e., the user position is approximated with the location of the RBS used for the telecommunication activity. This approximation implies that the user’s position within an RBS’s coverage area is unknown and that user tracking depends on the spatial distribution of antennas on the territory, which depends on population density. Nevertheless, mobile phone data may cover a large sample size on a national scale. An advantage of mobile phone data is its multidimensionality: CDRs also provide information about the social interactions between users; both CDRs and XDRs may be accompanied by socio-demographic information about the users (e.g., age, sex).

3.1.1 Available datasets. Since mobile phone data contain sensitive information [37, 123], they are not typically publicly available, and any data collected by a specific group of researchers may not be shared with other groups, making reproducibility difficult. Some companies launched initiatives, e.g., data challenges, to release large scale CDRs for research upon requests, such as the Telecom Italia’s Big Data Challenge (TBDC) [8].

Nevertheless, some aggregated information extracted from mobile phone data has been publicly released in the last few years. For instance, the WorldPop project [164] integrates mobile phone data with censuses, surveys, and other data sources to estimate the population density worldwide with a spatial granularity of $100\text{m} \times 100\text{m}$ cells.

The provided dataset is especially relevant for low-income and mid-income countries in which official surveys and census data may be inconsistent and with an inadequate spatial granularity [163].

Du et al. [41] make publicly available three datasets about the displacements of two million users in the Changchun over one week: 1) the temporal network, describing the last location visited by each user per each hour of the day; 2) the mobility network, describing the number of users moving between a pair of RBSs for every hour of the day; 3) a matrix of the distances between locations, since they do not provide a precise geographic position of the locations. Similarly, Du et al. in [40] provides, for one week, hourly aggregated movements of almost three million users among 167 administrative divisions in Sangliao Basin, northeast China ($\approx 20 \text{ km}^2$).

TBDC [8] publish three multi-source datasets containing mobile phone activities (aggregations of CDRs and XDRs) over two months in Milan and the Province of Trentino, Italy. The first dataset describes the incoming and outgoing calls/messages and internet traffic data activity for each cell of a squared tessellation. The second dataset depicts the interaction between the cells in Milan/Trentino and other Italian provinces. The third dataset provides the directional interaction strengths between pairs of cells in Milan and Trentino.

Other mobility datasets are available on-site upon the approval of a project proposal. For example, the EU-funded research infrastructure SoBigData [66] opens regular calls for projects proposal on datasets of various types, including mobility ones [4]. In particular, the SoBigData catalog [150] includes CDRs regarding Tuscany, the city of Pisa, and the city of Rome, Italy.

3.2 GPS traces

Global Navigation Satellite Systems (GNSS) are an essential source of human mobility data. A navigation satellite system uses satellites to provide geo-spatial positioning, allowing electronic receivers to determine their location (longitude, latitude, and altitude) and time, using signals transmitted along a line of sight from satellites. The US Global Positioning System (GPS), the Russian Global Navigation Satellite System (GLONASS), the Chinese BeiDou Navigation Satellite System (BDS) and the EU Galileo are all examples of GNSS. Among these systems, GPS is by far the most popular one, and GPS receivers are ubiquitous in many tools of everyday life, such as mobile phones [3, 160, 208], vehicles [56, 118, 121], vessels [140, 151, 172], and wearable devices [136]. On mobile phones, the GPS receiver is activated by apps that require the user's position (e.g., Google Maps). On vehicles, the GPS device automatically turns on when the vehicle starts, sending positions to a server with a frequency of a few seconds. The precision of GPS receivers varies from a few centimeters to meters, depending on the device's quality and the errors generated by the system [24]. Moreover, GPS cannot track the devices in enclosed spaces, such as buildings and tunnels. A typical GPS trace is a set of tuples (u, t, lat, lng) where u is a user, t is a timestamp of the measurement and lat, lng are the position's latitude and longitude. GPS traces may require several preprocessing tasks aimed to mitigate errors and extract meaningful semantics. For example, since GPS traces are dense sequences of spatio-temporal points, they do not explicitly define semantic locations, which must be inferred through specific preprocessing techniques [50, 206, 207].

3.2.1 Available datasets. GeoLife [208] is a publicly available dataset describing the GPS trajectories of 182 users over 4.5 years, collected using different devices (e.g., GPS receivers and mobile phones) every 1-5 seconds or 5-10 meters. GeoLife covers a broad range of users' outdoor movements, from life routines like go home and go to work to entertainment and sports activities. Each point in a GeoLife's trajectory contains latitude, longitude, altitude, and the timestamp. Moreover, the user's transportation mode is also available for most of the trajectories.

In 2013, OpenStreetMap (OSM) released a GPS dataset that contains information from seven years of activity, corresponding to almost three billion GPS points [114]. The dataset describes GPS trajectories, uploaded by voluntary users, which describe movements with different transportation means. The last updated version of the dataset dates back to April 2013, but it is possible to download more recent GPS traces using OSM's APIs. The

geographic distribution of GPS points is denser in specific countries and regions: 20% of the world contains 75% of the measurements.

Other public datasets provide information about the trips of GPS-equipped taxis in several cities. Piorkowski et al. [127] provide the trajectories, sampled on average every 10 seconds, of taxis in San Francisco, in May 2008. Each point of a trajectory consists of the taxi's identifier, the latitude, the longitude, the timestamp, and the occupancy. Bracciale et al. [18] provide trajectories of taxis in Rome, Italy, in which points are gathered on average every 7 seconds. Each point contains the taxi's identifier, the latitude, the longitude, and the timestamp. Moreira et al. [109] (ECML/PKDD Challenge) provide the trips of taxis in Porto, Portugal, in which points contain the latitude, the longitude and a timestamp indicating when the trip started. Data are collected approximately every 15 seconds. For each trip, the dataset provides several auxiliary information, such as the trip's typology (e.g., dispatched from the central, demanded to the operator, requested to the driver), the stand from which the taxi departed, and an identifier of the passenger's phone number. The Taxi and Limousine Commission of New York City collected a dataset on yellow and green taxis operating in the city starting from 2009 [167]. The dataset provides information on pick-up and drop-off dates/times and locations, trip distances, itemized fares, rate types, payment types, and driver-reported passenger counts.

The T-Drive dataset [205] describes the trajectories of about 10,000 taxis in Beijing, China, for one week. Points are sampled every 177 seconds and contain the taxi's identifier, the latitude, the longitude, and the timestamp. Zhang et al. [201] create a squared tessellation on New York City and Beijing and, for each tile, provide the incoming and the outgoing flows. Beijing's flows are captured based on taxis' GPS signal; the New York City ones are based on the city's bike-sharing system.

Citi Bike by Lyft [12] provides a dataset describing the trips between bike-sharing stations in New York City. Each record describes the stations where the trip started and ended when it took place and the stations' coordinates. There are similar open datasets for other cities, such as Washington DC [13].

The Mobile Data Challenge dataset (MDC) [96] describes the trajectories of 185 participants of the Lausanne Data Collection Campaign, collected from mobile phones [88]. The dataset offers various information (e.g., calendar logs and data from accelerometers), including two files describing the individuals' mobility through GPS receivers and Wireless Local Area Networks (WLANs). Each record in the file with the GPS tracks describes the user's identifier, latitude, longitude, altitude, timestamp, speed, heading direction, and accuracy. The WLANs file provides a set of records describing the user's identifier, a timestamp, the first three bytes of the device's MAC address, and the access points' location.

Other GPS datasets are available on-site upon the approval of a project proposal, such as tracks of private vehicles and traces provided by voluntary individuals traveling in Italy, provided by SoBigData [4, 150].

Recently, to take countermeasures for the COVID-19 pandemic, companies such as Cuebiq and SafeGraph are providing free access upon request to their data.³ The former allows researchers to access mobility insights such as traveler analysis, home switcher trend, and a mobility dashboard. SafeGraph allows for accessing three datasets: the first two contain information about points of interest (POIs), e.g., name, category, geometry, the third one about traffic patterns, e.g., how often people visit a place, how long they stay, where they came from.

3.3 Social Media Data

Nowadays, users' posts on social media (e.g., photos, text, videos) can be geotagged, i.e., associated with a geographic location and time. The presence of spatial and temporal information allows the reconstruction of users' trajectories from the sequence of published posts. Some platforms like Twitter provide two geotagging formats: the post's precise geotag (i.e., a latitude and longitude pair, a format recently removed) or the position of a predefined location suggested by the platform (e.g., a city, an area, a restaurant). In other platforms like Foursquare

³Cuebiq: cuebiq.com/visitation-insights-covid19/, SafeGraph: safegraph.com/covid-19-data-consortium

and Facebook, users can check-in in predefined locations called venues, i.e., POIs that provide information about social, cultural, and infrastructural components of a geographic area (e.g., cities, shops, museums). A venue is associated with a physical location (latitude and longitude pair) and textual information (a description of the place or the activities related to the place) and can follow a hierarchical categorization that provides different levels of detail about the activities (e.g., Food, Asian Restaurant, Chinese Restaurant) [10]. In Yelp, whenever a user publishes a comment or a photo, they can associate it with a specific geolocated business (e.g., restaurant). Similarly, Flickr users can post and geotag photos, which may be associated with predefined locations as well as specific coordinates. In general, a geotagged record describes the posting user's identifier, the resource identifier (e.g., post, tweet, photo), the time of posting, and, depending on the platform, the venue identifier/category or a location as a string (e.g., Statue of Liberty, New York) or a latitude and longitude pair.

For most of the social media platforms, geotagged posts are downloadable through their APIs. APIs impose limitations on the number of downloadable posts and queries per day or require authorization from the platform's users to download the data. Users' location is available only when they post something or check-in into a venue, leading to a data sparsity problem. Nevertheless, social media data bring the advantage that an objective definition of location is available, facilitating the data preprocessing phase [35].

3.3.1 Available datasets. Datasets about check-ins on social media platforms that are not active anymore, such as Gowalla and Brightkite, are freely available. Gowalla was a location-based social network platform in which, similarly to Foursquare, the users were allowed to check-in in the so-called spots (venues) through a website or the app. The related dataset [29] consists of more than six million check-ins over one year and a half from February 2009 to October 2010. Each check-in describes the user identifier, the location identifier, the latitude and longitude pair, and a timestamp. The dataset also provides information about the users' friendship network, which contains about 200,000 nodes and one million edges [29]. In Brightkite, another platform that is not active anymore, users were allowed to check-in in POIs, to specify who is nearby at the moment and who went to a POI before. The dataset contains almost 4.5 million check-ins from April 2008 to October 2010 and the users' friendship network with about 60,000 nodes and 220,000 edges [29].

Yang et al. [190] provide a Foursquare dataset collected over ten months and containing about 230,000 check-ins in New York City and 575,000 in Tokyo. Each check-in record describes the user's identifier, the venue's identifier and its category, latitude, longitude, and timestamp. Additionally, the same authors also collected check-ins on a global scale from April 2012 to September 2013, involving 415 cities in 77 countries [187, 188]. This dataset also provides the country code of the venue and information on the 415 cities involved in the study (latitude, longitude, country code and name, type of city). They also offer the possibility to associate, for about 18,000 users in New York City and 12,000 in Tokyo, with the related gender, the number of following and follower users on Twitter [189]. Another dataset collected through Foursquare APIs is introduced in [47] and contains check-ins of 16,000 users over one year in New York City.

The Yahoo Flickr Creative Commons 100 Million Dataset (YFCC100M) [165] contains 100 million open-license media objects (photos and videos) collected between 2004 and 2014 from the popular service Flickr. Each record describes the camera's model used to take the photo or video, a set of tags, and the timestamp when the photo or video was made. For about 48 million photos and 100,000 videos, the geographic location is also available as latitude and longitude pair, either inserted manually by the user or through the device's GPS receiver.

Twitter provides several open datasets, in which location is usually expressed as a semantic point of interest either suggested by the platform (e.g., Empire State Building, NYC) or typed by the users (e.g., Home), or as a latitude and longitude pair. Geotagged tweets may be retrieved directly using Twitter APIs. For example, Zhang et al. [199] (GMove) provide a Twitter dataset describing 1.4 million tweets from August to November 2014 covering the area of Los Angeles. In 2020, some Twitter datasets with geotagged information have been

| | Ref. | Name | Items | Time span | Area | Access | Link (https://bit.ly/) |
|-------------------------|-------|---------------------|---------|-----------------------|--------------------------|-------------------|--|
| Phone | [8] | TBDC | - | 2 months | Milan & Trento, Italy | public | TBCD-2 |
| | [164] | WorldPop | - | 20 years | World | public | WorldPop-Data |
| | [41] | Changchun | 2M | 1 week | Changchun, China | public | Changchun-Data |
| | [40] | Songliao Basin | 3M | 1 week | Sangliao Basin, China | public | Songliao |
| GPS | [208] | GeoLife | 182 | 4,5 Years | Asia | public | Geolife |
| | [205] | T-Drive | 10k | 1 Week | Beijing, China | public | T-Drive-Data |
| | [114] | OSM | - | 7 years | World | public | osm_gps |
| | [201] | ST-ResNet taxis | - | 4, 6 months | Beijing, China | public | ST-ResNet |
| | [201] | ST-ResNet bikes | - | 6 months | New York City, USA | public | ST-ResNet |
| | [127] | Taxi San Francisco | 500 | 30 days | San Francisco, USA | upon registration | TaxiSF |
| | [18] | Taxi Rome | 320 | 1 months | Rome, Italy | upon registration | TaxiRome |
| | [109] | ECML-PKDD taxi | 441 | 9 months | Porto, Portugal | public | TaxiPorto |
| | [167] | Taxi New York City | - | From 2009 | New York City | public | TaxiNYC-2 |
| [96] | MDC | 185 | 2 years | Lausanne, Switzerland | upon request | MDC-2 | |
| Social Media & checkins | [29] | Gowalla | 196k | 20 months | California & Nevada, USA | public | GowallaData |
| | [29] | Brightkite | 58k | 30 months | - | public | Brightkite |
| | [190] | Foursquare | 800k | 10 months | NYC, Tokyo, World | public | Foursquare-Data |
| | [47] | DeepMove | 16k | 1 Year | New York City | public | DeepMove |
| | [193] | Yelp | 200k | - | 4 countries | upon registration | YelpData |
| | [165] | YFCC100M | 100M | 10 Years | World | upon request | YFCC100M |
| | [199] | GMove | 1.4M | 4 Months | Los Angeles | public | SERM-Repo |
| | [112] | GeoCoV19 | 43M | 90 Days | World | public | GeoCoV19 |
| | [12] | New York City bikes | - | from 2013 | New York City, USA | public | BikeNYCData |
| | [13] | Washington DC bikes | - | from 2010 | Washington DC , USA | public | BikeWashington |
| Auxiliary | - | Open Transport Map | - | - | World | public | OTM-DATA |
| | - | World Meteo. Org. | - | - | World | public | WMO-DATA |
| | - | Weather Underground | - | - | World | public | WUnderground |
| | - | EU Statistics | - | - | European Union | public | EUCensusUB, EUDataPortal, EUUrbanAtlas |
| | - | UN Statistics | - | - | World | public | UNCensusHub |
| | - | OECD | - | - | World | public | OECD CensusHub |

Table 1. Mobility datasets available for research. For each dataset, we provide a reference to the paper introducing it, the number of items (users or points) in the dataset (symbol “-” indicates that the dataset is aggregated or that the number is not available), its time span, area covered, and access type (public, upon registration, upon request), and the link to download it.

released to track the COVID-19 pandemic [49, 112]. A comprehensive list of Twitter datasets is available at github.com/shaypal5/awesome-twitter-data.

Yelp released two datasets containing information about check-ins in 174,000 businesses for 11 metropolitan areas over four countries [193]. One dataset describes the geographic position of Yelp businesses, the other one describes the check-ins, each associated with a business identifier and timestamp but without the user’s identifier that generated it.

3.4 Auxiliary Data

To add semantic to human mobility, deep learning models often use data describing the context in which movements take place. These auxiliary data may represent vehicular traffic, weather conditions, and census and administrative data. In what follows, we discuss these data’s characteristics and summarize some data sources in Table 1.

3.4.1 Traffic data. Sensors provide various information about urban traffic (e.g., the number of vehicles on the streets, their average speed) at various temporal aggregations. For example, cities like Turin, Italy Hamburg, Germany and New York City, US, have open datasets containing traffic information with temporal scales varying from minutes to days. The Open Transport Map project allows routing and visualization of traffic volumes in the

EU. In general, traffic records contain a timestamp of the measurement and the number of vehicles, bikes, or pedestrians passed through a road segment between two consecutive measurements.

3.4.2 Environmental data. Weather data are often used in crowd flow prediction because the meteorological conditions significantly impact how people move. There are many datasets on the open data portals of regions, states and municipalities regarding the meteorological conditions, and there are also repositories that offer a global-scale perspective. In particular, the World Meteorological Organization allows downloading the forecast and climatologist information for almost all the nations. Weather Underground is a popular tool to retrieve temperature, dew point, humidity, wind speed, pressure, precipitation and weather conditions on a global scale, offering the possibility to explore different periods depending on the station and the city of interest.

3.4.3 Census and Administrative Data. Census data provide information about the mobility flows, the socio-demographic characteristics, and the socio-economic status of a geographic region at various spatial scales [6, 173]. They are periodically collected through surveys by public institutions and statistical bureaus every five or ten years and provide information about households' workplace, current and previous residence, and household members. Census and administrative data are available from the websites of the national and international public entities and statistical bureaus responsible for the data collection and processing. The UN and the OECD provide portals with census data at national and international levels. For a list of available census data sources and detailed discussions on how they are used for human mobility studies, the reader may refer to [6, 175] and to the website of the UN statistics division⁴ and the OECD⁵. For example, USCB collects data on commuting trips between counties in the US, in companion with further information on counties' spatial distribution and socio-demographic data. Similarly, ONS collects commuting and migration flow for the UK at different spatial resolutions, and the EU CensusHub portal provides census data of all EU countries. When not available on an open portal, commuting data are available to researchers on request from national statistics institutes. Census data portals often contain land use data, which indicate the use class of each urban zone in a region, e.g., residential, commercial, and manufacturing. In this regard, the Urban Atlas on the EU Open Data Portal contains land use data standardized in 20 land use classes, covering cities of 100,000 inhabitants or more.

4 TASKS

In this section, we discuss the most relevant DL approaches that solve next-location prediction, crowd flow prediction and trajectory generation. For each task, we define the problem and discuss the papers that address it. In Table 2, we provide detailed information for each approach, highlighting the DL techniques, the evaluation metrics, the public dataset used for the experiments, and a link to the implementation (if any).

4.1 Next-Location Prediction

Why it is an important problem. Predicting people's movements impact many areas such as an individual's health and mobility patterns [9, 23], well-being conditions [122], traffic congestion [145], travel recommendation, location-aware advertisements, geomarketing and recommendation of friends in social network platforms [20, 179, 203, 204, 210]. Next-location predictors can help policymakers organize their public transportation network, urban planners decide a city's future developments, and transportation companies provide citizens with a better service in terms of traffic reduction and ease of mobility.

Problem Definition. Next-location prediction consists of forecasting the next location an individual will visit in the future, given their historical mobility data. This problem can be treated in two ways: (i) as a multiclass classification task, by tessellating a geographical space and predicting the next visited tile; (ii) as a regression task,

⁴https://unstats.un.org/home/nso_sites/

⁵<https://stats.oecd.org/>

| | Reference | Name | Year | Model | Evaluation | Dataset | Code (https://bit.ly) |
|--------------------------|----------------------|------------|--------------|----------------------------|---|--------------------|--|
| Next-Location Prediction | Chen et al.[28] | DeepJMT | 2020 | GRU, FC, Encoder | ACC@k | [186] | - |
| | Yang et al.[185] | Flashback | 2020 | Attention, RNN | ACC@k | [29] | Flashback-1 |
| | Ebel et al.[43] | - | 2020 | RNN | Distance | [109, 127] | - |
| | Rossi et al.[135] | - | 2019 | Attention, LSTM | Distance | [109, 127, 167] | - |
| | Gao et al.[59] | VANext | 2019 | CNN, GRU | ACC@k | [29] | - |
| | Kong et al.[90] | HST-LSTM | 2018 | LSTM | ACC | - | HST-LSTM |
| | Lv et al.[104] | T-CONV | 2018 | CNN | Distance | [109] | T-CONV |
| | Feng et al.[47] | DeepMove | 2018 | Attention, RNN | ACC | [47] | DeepMove |
| | Yao et al.[191] | SERM | 2017 | LSTM | HR@k | - | SERM-Repo |
| | Liu et al.[102] | ST-RNN | 2016 | RNN | Rec@k, F1@k, MAPE, AUC | [29, 158] | STRNN |
| De Brébisson et al.[36] | - | 2015 | FC | Equirectangular Distance | [109] | next-loc-1 | |
| Crowd Flow Prediction | Ren et al.[131] | HIDLST | 2020 | LSTM, ST-ResNet | RMSE | [201] | - |
| | Tian et al.[166] | LDRSN | 2020 | CNN, Attention | RMSE, MAPE, MAE | [12, 167] | - |
| | Yuan et al.[197] | MV-RANet | 2020 | CNN, Attention, Res. | RMSE, MAPE | [201] | - |
| | Liu et al.[101] | ATFM | 2020 | ConvLSTM | RMSE | [201] | ATFM-2 |
| | Li et al.[98] | ST-DCCNAL | 2019 | CNN, Attention, LSTM | RMSE | [201] | ST-DCCNAL |
| | Sun et al.[161] | MVGCN | 2019 | GCN | RMSE, MAE | [12, 13, 167, 201] | - |
| | Lin et al.[100] | DeepSTN+ | 2019 | CNN, Res. | RMSE, MAE | [12] | DeepSTN |
| | Du et al.[39] | DST-ICRL | 2019 | CNN, LSTM, Res. | RMSE, MAE | [201] | DST-ICRL |
| | Ai et al.[2] | - | 2018 | ConvLSTM | RMSE, MAE | - | - |
| | Yao et al.[192] | STDN | 2018 | CNN, LSTM, Attention | RMSE, MAPE | [12] | STDN-2 |
| | Jin et al.[80] | STRCN | 2018 | CNN, LSTM | RMSE | [201] | - |
| Zonoozi et al.[211] | PCRN | 2018 | ConvGRU, CNN | RMSE | [201] | - | |
| Zhang et al.[201] | ST-ResNet | 2017 | CNN, Res. | RMSE | [201] | ST-ResNet | |
| Trajectory Generation | Feng et al. [48] | MoveSim | 2020 | GAN, self-attention CNN | distances, r_g , $p(r, d)$, DailyLoc, G-rank, I-rank | [208] | MoveSim |
| | Huang et al. [72] | SVAE | 2019 | VAE, LSTM | MDE | - | - |
| | Ouyang et al. [115] | Ouyang GAN | 2018 | WGAN, CNN | $p(r)$, $p(r, t)$, $p(r, d)$, $p(r, d_{total})$, $p_{d_{total}}$, location frequency | [96] | - |
| | Kulkarni et al. [94] | - | 2018 | RNN, GAN, copula | visitation frequency, statistical similarity, privacy tests | [96] | - |
| | Yin et al. [194] | - | 2018 | GAN, FC | reconstruction error, utility loss | [127] | - |
| | Liu et al. [103] | trajGANs | 2018 | GANs | - | - | - |

Table 2. List of relevant papers tackling next-location prediction, crowd flow prediction and trajectory generation.

predicting the latitude and longitude of the next visited location. Formally, let u be a user, T_u their trajectory, and $p_k \in T_u$ u 's current location, next-location prediction is the problem of predicting the next destination p_{k+t} of u . In the multiclass classification task, p_{k+t} is the identifier of the next tile; in the regression task, $p_{k+t} = (x_{k+t}, y_{k+t})$, where x and y are the location's geographic coordinates. In a variant of next-location prediction, given the user's semantic trajectory T_u and their current location $p_k \in T_u$, the purpose is to forecast the POI p_{k+t} u will visit. In general, next-location predictors output a ranking of the locations that are most likely to be the destinations of u .

Why it is a challenging problem. Human mobility is characterized by a high degree of regularity and hence of predictability [42, 154], which is mainly encoded in the temporal order of the visitation patterns. However, humans decide where to go next based on many other aspects, such as transportation modality, traffic, weather conditions, and social contacts. Thus, next-location prediction poses two main challenges: (i) the design of a dense representation of temporal and spatial characteristics of human movements; (ii) the need for combining efficiently heterogeneous data sources to model multiple factors influencing human displacements.

Traditional approaches. Next-location prediction has been widely explored prior to the deep learning explosion and generally tackled using probabilistic or pattern-based approaches, which can work with a reasonably small amount of data [20, 204]. In a seminal work, Calabrese et al. [22] propose a probabilistic model that combines people's trajectories and geographical features such as land use, POIs, and distance of trips. Other approaches

use Markov models. Ashbrook et al. [5] cluster GPS data into meaningful locations and incorporate them into a Markov model to predict individuals' future movements. Gambs et al. [57] introduce a Mobility Markov Chain (MMC) in which states represent POIs and transitions between states correspond to a movement between two POIs. A limitation of Markov models is that they exploit the current location only to predict the next one. To overcome this problem, Gambs et al. [58] extend MMC into n -MMC considering the n previous visited locations. Among the pattern-based approaches, Monreale et al. [107] develop a trajectory pattern mining algorithm to represent movement patterns as sequences of regions frequently visited with a typical travel time. Although traditional approaches have some degree of interpretability and can achieve good performances with a small amount of data, they have substantial limitations. Notably, they require a considerable effort in feature engineering and have limited memory, making it hard for them to capture long-range temporal dependencies [141].

DL approaches. De Brébisson et al. [36] use an FC to predict taxi's passenger drop-off locations. The input data consist of trajectories represented as a variable-length sequence of GPS points and other meta-information, such as departure time, driver identity, and client information. The model achieves good performances on the dataset of taxis in Porto [109] in terms of equirectangular distance to the actual visited location. However, it cannot take into consideration the temporal dimension of the mobility data.

ST-RNN (Spatial Temporal Recurrent Neural Networks) [102] overtakes this issue by extending RNN with time- and spatial-specific transition matrices. Each RNN's layer learns an upper and lower bound for the temporal and spatial matrices through linear interpolation. The predicted location is the one on the top of a ranking of all possible locations. The model is evaluated on the datasets of Gowalla [29] and the Global Terrorism Dataset [158] using F1-score, Rec@k, MAPE, and AUC.

DeepMove [47] is an attentional recurrent network for mobility prediction from lengthy and sparse trajectories. First, historical and current trajectories are passed to a multi-modal embedding module to create a dense representation of the spatio-temporal and individual-specific features. Historical trajectories are handled by an attention mechanism to extract mobility patterns, while a GRU handles current trajectories. The output of the multi-model embedding, the GRU, and the attention mechanism are concatenated and passed to an FC to predict an individual's next-location. DeepMove is evaluated, using ACC, on Foursquare data [47], mobile phone data, and a dataset from a popular Chinese social network platform.

HST-LSTM (Hierarchical Spatial-Temporal LSTM) [90] aims at predicting an individual's short-term next-location. First, the authors design ST-LSTM (Spatial Temporal LSTM), which combines a trajectory's spatial and temporal characteristics using an LSTM. ST-LSTM is then extended into HST-LSTM, which models periodic patterns using an encoder-decoder module. The encoder encodes the locations visited by a user in a given time span and area of interest. The decoder predicts the possible areas of interest the user will visit next. HST-LSTM is evaluated using ACC on private data from Baidu.

T-Conv [104] treats trajectories as images and handle them using CNNs to capture the spatial patterns at different spatial scales. The output of the CNN, the trajectory's starting datetime, and other personal information about the user are passed to an FC that handles the prediction. T-Conv is evaluated using the datasets of taxis in Porto [109] and the Haversine distance. Rossi et al. [135] propose an LSTM network equipped with a self-attention module to predict the coordinates of a taxi's next drop-off location. Locations are enriched with geographical data to describe the surrounding area of the location semantically. The model is tested using the Haversine distance and on the datasets of taxis in Porto [109], New York City [167], and San Francisco [127].

Another strand of research focuses on predicting the next POI an individual will visit using semantic trajectories. For example, SERM (Semantics-Enriched Recurrent Model) [191] relies on an embedding layer to represent the timestamp, the location, and the keywords of a social media post concisely. Both the user's trajectory and the embedding are fed into an LSTM responsible for predicting the next POI. SERM is evaluated using ACC@k on data from Foursquare posts in New York City [198] and tweets in Los Angeles [199].

In VANext (Variational Attention based Next Location) [59], the historical trajectories and the current one are embedded using two separate causal encoders to represent the semantic relationships among POIs. The encoded historical trajectories are passed to a CNN; the encoded current trajectory is passed to a GRU. The outputs of the CNN and the GRU are passed to an attention mechanism, which detects the most similar historical trajectory to the current one and passes it to an FC that predicts the individual’s next POI. VANext is evaluated using ACC@k on the datasets of Gowalla [29] and Foursquare for Singapore and New York City.

Flashback [185] is based on an RNN and the concept of “flashback”: a technique that, given a sparse semantic trajectory, predicts the next POI by looking for similar trajectories in terms of temporal characteristics. Flashback also uses an embedding to model the preferences of individuals to visit specific POIs. The outputs of the RNN and the embedding are passed to an FC that predicts the next visited POI. Flashback is evaluated using ACC@k on social media posts from Gowalla [29] and Foursquare.

DeepJMT (Deep Model for Joint Mobility and Time) [28] can predict an individual’s next POI as well as when they will visit it. The model is based on four pipelines: a sequential dependency encoder, a spatial context encoder, a periodicity context extractor, and a social-temporal context extractor. The sequential dependency encoder is a hierarchical GRU that takes as input an embedding of a user’s trajectories. The high-level GRU captures the transitions between trajectories; the low-level GRU models the transition within a trajectory. The spatial context extractor determines the dynamic influence of spatial neighbors, modeled as a graph in which nearest points influence the final prediction. The periodicity context extractor is an attentional GRU aiming at extracting periodicity patterns from an individual’s historical trajectories. The social-temporal context extractor leverages social relationships using an FC and pooling functions to facilitate both next-POI and time prediction. Finally, the outputs of the four modules are concatenated to generate the prediction. DeepJMT is evaluated using ACC@k on data from Foursquare in New York City [186], Tokyo [186] and Istanbul.

Ebel et al. [43] propose a model to predict a vehicle’s destinations and routes, given a partial trajectory and context data (e.g., day, time, weather). First, the area is tessellated and GPS points are assigned to these tiles using a k-d tree-based space partitioning method. The model is based on two main modules. The first module is an RNN that takes as input the mapped trajectory; the second module is an FC that takes as input the embedded contextual data. The two modules’ outputs are merged and passed to an additional FC that produces the individual’s probabilities to end their trip into a specific tile and the destination coordinates. The model is evaluated using the mean Haversine distance and the distance to the actual arrival point on the datasets of taxis in Porto [109] and San Francisco [127].

4.2 Crowd Flow Prediction

Why it is an important problem. Crowd flow prediction is the problem of predicting the incoming and outgoing flows of locations in a geographic region, usually split into tiles on a spatial tessellation [180, 207]. It is a crucial problem given its impact on several aspects of society, from public safety [207] to the definition of on-demand services [209], the management of land use [76], and traffic optimization [207]. Crowd flow predictors may help city managers and policymakers discover the traffic congestions in the city; people in business find potential areas of business investment; citizens improve travel plans and stagger the peaks of travel. Crowd flow prediction may also help prevent or mitigate dangerous situations, such as creating massive crowds of people streamed into a strip region, by sending out warnings or evacuating people in advance.

Problem Definition. Given an individual’s trajectory T_u , the set of cells (tiles) the trajectory intersects in a time interval Δt is:

$$q_{T_u}^t = \{(p_k \rightarrow t) \in \Delta t \wedge (p_k \rightarrow (x, y)) \in (i, j) | (i, j)\}, \quad (7)$$

where (i, j) indicates a cell on a $i \times j$ grid and p_k is the user u ’s current location, identified by the coordinates (x, y) . Let Q be the set of locations covered by all the individual trajectories and let $t - 1$, t , and $t + 1$ be three

consecutive time spans, the incoming flow to a location (i, j) is the number of the individuals that are in (i, j) at time t but were not in (i, j) at time $t - 1$. Similarly, the outgoing flow to location (i, j) is the number of individuals that are in (i, j) at time t and move to another location at time $t + 1$:

$$\text{in}_t^{(i,j)} = \sum_{T \in Q} |\{t > 1 | (i, j) \notin q_T^{t-1} \wedge (i, j) \in q_T^t\}|; \quad \text{out}_t^{(i,j)} = \sum_{T \in Q} |\{t > 1 | (i, j) \in q_T^t \wedge (i, j) \notin q_T^{t+1}\}|. \quad (8)$$

We can represent the flows of a region as a tensor $X_t \in R^{2 \times I \times J}$, where one dimension is associated with the in-flow $(X_t)_{1,i,j} = \text{in}_t^{(i,j)}$ and the other with the out-flow $(X_t)_{2,i,j} = \text{out}_t^{(i,j)}$. Therefore, crowd flow prediction is the task of predicting $X_{t+\Delta t}$ given the historical flows $\{X_t | 1, \dots, X_t | t\}$. The performance of crowd flow predictors is evaluated as the error (e.g., RMSE, MAE) between the empirical in- and out-flows and the predicted ones.

Why it is a challenging problem. Crowd flow prediction is challenging because it requires dealing with both spatial and temporal dependencies. Regarding the spatial dependencies, a model should consider that a region's out-flow may affect the in-flows of both near and far regions. Concerning the temporal dependencies, crowds are characterized by temporal closeness, trends, and periodicity. Temporal closeness marks the dependencies between events that are close in time; trends highlight patterns that repeat over time (e.g., weekends and working days); periodicity captures the repetitive nature of relevant events (e.g., rush hours in the morning). Moreover, crowd flow patterns are affected by external factors such as weather conditions and holidays.

Traditional approaches. Crowd flow prediction is usually addressed using classic time-series prediction models based on autoregression (AR). Some examples are the Autoregressive Moving Average (ARMA) designed by Box et al. [17], the Autoregressive Integrated Moving Average (ARIMA) introduced in [97, 108], and other variants like the Stationary and Seasonal ARIMA (SARIMA) [178], vector ARMA [83] and space-time ARIMA [84]. Unfortunately, ARMA and ARIMA have the same limitations as autoregressive models: since they can make predictions only out of stationary time-series that do not statistically change overtime, they cannot accurately predict new events. Other models such as SARIMA, vector ARMA and space-time ARMA are designed to overtake this assumption, but they present other issues. For instance, the predictive performance of SARIMA decreases when dealing with patterns with long seasonal periods. In general, the AR-based time-series predictors have difficulties in handling spatial dependencies, making them unsuitable for crowd flow prediction. For this reason, AR-based models are usually employed as a baseline for DL crowd-prediction models.

DL approaches. DL-based solutions overcome the limitations of AR methods for time-series prediction [38, 54, 81, 200] and, in the last years, they have been profitably used for crowd flow prediction.

Most of the approaches in the literature exploit the capability of CNNs to capture spatial-structural information and the relationships between near-by and far-away zones in the region of interest. This is crucial because the in/out-flow of an area may affect the in/out-flow of a far-away part of the region. For instance, by taking a car or other transportation means such as buses or cabs, an individual may travel from the southern part of a city to the northern one, hence influencing in-flows and out-flows in distant neighborhoods of the city. To evaluate the predictors, most of the authors use RMSE as the evaluation metric and [201] as the input dataset. The latter contains information on taxi flows in Beijing and bikes in New York City with a squared tessellation of sizes 32×32 and 16×8 tiles, respectively. In the following descriptions, we only mention the usage of different datasets and additional evaluation metrics.

In their seminal work, Zhang et al. propose ST-ResNet [201], which consists of three modules that rely on convolution layers and residual units to capture trends, periodic patterns, and temporal closeness. The modules' output is combined with the output of an FC that deals with external factors such as weather conditions.

Many works in the literature combine CNNs with RNNs to exploit the latter's capability to deal with temporal patterns. STRCN (Spatio-Temporal Recurrent Convolutional Network) [80] uses three CNNs to capture close, short-term (daily influence), and mid-term (the difference between workdays and weekends) spatial patterns. The output of the CNNs is fed into three LSTMs, which handle temporal dynamics. STRCN also uses external

features, such as weather conditions and features to distinguish between workdays and holidays, through an FC. The output of the FC and the LSTMs are combined.

STDN (Spatial-Temporal Dynamic Network) [192] consists of two CNNs: the first one captures the local spatial dependencies based on the similarities of historical traffic volumes to uncover the flows; the second CNN captures the traffic flows. The outputs of the two CNNs are pairwise multiplied and summed with an FC's output that handles external features (e.g., weather events). Moreover, STDN uses three LSTMs to capture the temporal dependencies of historical data describing the crowd flows. CNNs and LSTMs work on two separate pipelines, the outputs of which are summed together and forwarded to another LSTM with an attention mechanism that analyzes the temporal dynamics of the current day. Finally, the output of this latter LSTM is passed to an additional FC to perform crowd flow and traffic prediction. Experiments are conducted on the New York City's bikes dataset [12] and on a dataset of taxis' flows in New York City [167], using a squared tessellation of 10×20 tiles. The authors also use MAPE to evaluate the model.

DST-ICRL (Deep Spatio-Temporal with Irregular Convolutional Residual Network) [39] combines convolutional residual units with LSTMs to capture the irregular properties of traffic flows in different transportation lines. Similarly to STDN [192] and ST-RESNET [201], DST-ICRL uses three pipelines to uncover daily, weekly, and recent spatio-temporal dynamics and handles external features using an FC. In the experiments, the authors use two private datasets of check-ins from e-cards on buses and subways in Beijing with a 128×128 squared tessellation. The metrics for the evaluation are RMSE and MAE.

Another category of crowd flow predictors introduces the attention mechanism. ST-DCCNAL (Spatio-Temporal Densely Connected Convolutional Networks and Attention LSTM) [98] uses convolutional layers combined with an attentional LSTM to simplify the selection of the inputs. The authors use DenseNet [73] to cope with the spatial patterns and FCs to deal with the external features. The outputs of DenseNet and the FCs are fed into an attentional LSTM to extract temporal patterns and make the prediction.

MV-RANet (Multi-View Residual Attention Network) [197] uses two pipelines to deal with spatio-temporal patterns and mobility patterns. The first pipeline models the closeness, the periods, and the trends of crowd flows using three attention residual networks, the outputs of which are fused and passed to a convolutional layer. The output of the convolutional layer is then passed to an FC. The second pipeline captures the mobility patterns in the data, generating three graphs: one for the transition probability, one for the transition distance, and one that mimics the flow patterns. The three graphs are then encoded using Node2Vec [67], an algorithmic framework that learns a continuous feature representation of the nodes of a graph, and passed to an FC to extract relevant mobility patterns. The outputs of the FC handling the graph representation and the FC that handles the spatio-temporal patterns are fed into an additional FC responsible for making the prediction. The experiments are conducted on the flows of taxis in Beijing [201] with a squared tessellation of size 32×32 and private mobile phone data (CDRs) for the city of Sanya using an 85×110 squared tessellation. The metrics adopted to evaluate the proposed framework are RMSE, MAPE, and MAE.

LDRSN (Local-Dilated Region-Shifting Network) [166] consists of five modules. The first one is a convolutional residual unit that handles local spatial dependencies; the second one uses dilated units to deal with distant spatial dependencies. A k -dilated unit is a convolution that captures the correlation of two regions with a distance of k . The outputs of these two modules are fused and forwarded to two other modules: one handles long-term temporal dependencies, the other deals with short-term temporal patterns. The long-term module consists of three pipelines with consecutive convolutional layers, each followed by attention LSTMs. A single ConvLSTM handles the short-term patterns. The outputs of the two temporal modules are fed into a final module: as a first step, it sums the outputs of the two temporal modules and forwards the result to a convolutional layer to make the prediction. The model is evaluated on the dataset of bikes' [201] (with a 16×8 squared tessellation) and taxis' in New York City [167] (with a 10×20 squared tessellation) using MAPE, RMSE, and MAE.

To capture long-range spatial dependencies, DeepSTN+ (Deep Spatio Temporal Network Plus) [100] replaces the traditional residual units and the convolutional layers with ResPlus and ConvPlus. ResPlus units employ a ConvPlus layer and a standard convolutional layer to capture distant spatial dependencies. The idea beyond a ConvPlus layer is to separate the channels of the input matrix and use an FC to capture the long-range spatial dependencies among each pair of regions. Finally, DeepSTN+ uses an average pooling layer before the FC to reduce the number of parameters. Another peculiarity of DeepSTN+ is that it uses temporal factors and the distribution of POIs to gain prior knowledge of the crowd flows. The experiments are conducted on the dataset of bikes in New York City [12] with a 21×12 squared tessellation and a private dataset from the most popular social network vendor in China with a 19×21 squared tessellation. DeepSTN+ is evaluated using RMSE and MAE.

Some other models address slightly different definition of crowd flow prediction [2, 161, 211].

PCRN (Periodic Convolutional Recurrent Networks) [211] solves the problem of predicting the distribution of presences in a city. The authors use a pyramidal model made of three ConvGRUs (which has both the advantages of CNNs and GRUs) with an external module that captures the patterns' periodicity by memorizing the periodic representations learned by the stacked ConvGRUs. The authors propose three different ways to retrieve and update the periodic patterns: using a sequential periodic representation, using an estimated average of periodic representation, adopting a temporally ordered representation. The outputs of the periodic module and the ConvGRUs are fused.

Ai et al. [2] aim to predict the short-term distribution of features that describe the movements of bikes of a dockless bike-sharing system. They rely on ConvLSTMs to address the spatial and temporal dependencies. ConvLSTMs take as input a spatio-temporal sequence composed of the number of bicycles in an area, the distribution uniformity, the usage distribution, and the time of the day to predict their values in the near future. The authors evaluate their model using private datasets from two bike-sharing companies in Chengdu, China. The metrics used for the evaluation are the RMSE and the MAE.

MVGCN (Multi-View Graph Convolutional Network) [161] solves the problem of predicting the origin-destination matrix representing the flows between urban areas. It handles the external features (e.g., weather data) with two FCs, which deals with weather information and meta-information such as time and day of the week. The authors select key time snapshots to process graphs representing recent, daily, weekly, monthly and quarterly mobility flows. Each node in these graphs represents a region with time-varying flows. The graphs are forwarded to five graph convolutional networks and the outputs of the seven networks (five graph convolutional networks and two FCs for the external features) are fused using a multi-view fusion mechanism. The fusion module's output is fed into an additional FC that outputs the predicted graph, in which each node is a region and the links are the predicted flows. The experiments are conducted on the dataset of bikes [12] and taxicabs [167] in New York City and on a dataset of bikes in Washington D.C. [13], using 120 irregular tiles and the dataset of taxicabs in Beijing [201] using a spatial tessellation with 100 irregular tiles. In both cases, RMSE and MAE are used to evaluate the performance of the models.

4.3 Trajectory Generation

Why it is an important problem. The goal of generative models of human mobility is to generate synthetic trajectories with realistic mobility patterns [6, 48, 70, 85, 146, 175]. The generated synthetic trajectories must reproduce a set of spatial and temporal mobility patterns, such as those presented in Section 2.2. The use of generative mobility models is crucial in many applications. First, synthetic trajectories are useful to the performance analysis of networking protocols such as mobile ad hoc networks, where the displacements of network users are exploited to route and deliver the messages [70, 85, 168]. Second, synthetic trajectories are fundamental for urban planning, what-if analysis, and computational epidemiology, e.g., simulating changes in urban mobility in the presence of new infrastructures, epidemic diffusion, terrorist attacks, or international

events. Furthermore, generative models are a viable solution to protect geo-privacy of trajectory data [53, 106]: while disclosing real data requires a hard-to-control trade-off between uncertainty and utility, synthetic records that preserve statistical properties may achieve in multiple tasks comparable performance to real data.

Problem Definition. A generative mobility model M is any algorithm able to generate a set of n synthetic trajectories $\mathcal{T}_M = \{T_{a_1}, \dots, T_{a_n}\}$, which describe the movements, during a certain period of time, of n independent agents a_1, \dots, a_n . The synthetic trajectory generated for a single agent a_i should be in the form of Definition 2.1, i.e., a time-ordered sequence $T_{a_i} = \langle p_1, p_2, \dots, p_k \rangle$ composed by spatio-temporal points, describing the k locations visited by a_i . The realism of M is evaluated with respect to:

- (1) A set of spatial patterns (s_1, \dots, s_{m_s}) and temporal patterns (t_1, \dots, t_{m_t}) $\mathcal{K} = \{s_1, \dots, s_{m_s}, t_1, \dots, t_{m_t}\}$ (see Section 2.2). The patterns refer to the distributions of individual measures, which quantify aspects related to the mobility of a single individual (e.g., radius of gyration, mobility entropy), or collective measures, which quantify aspects related to the mobility of a region as a whole (e.g., OD matrices). A realistic \mathcal{T}_M is expected to reproduce as many mobility patterns as possible.
- (2) A set $\mathcal{X} = \{T_{u_1}, \dots, T_{u_m}\}$ of real mobility trajectories corresponding to m real individuals $u_1 \dots u_m$ that move on the same region as the one on which synthetic trajectories are generated. Generally, a portion $\mathcal{X}_{\text{train}} \in \mathcal{X}$ is used to train M or to fit its parameters. The remaining part $\mathcal{X}_{\text{test}}$ is used to compute the set \mathcal{K} of patterns, which are compared with the patterns computed on \mathcal{T}_M .
- (3) A function D that computes the dissimilarity between two distributions, such as the KL divergence or the JS (Section 2.7.6). Specifically, for each measure in $f \in \mathcal{K}$, $D(P_{(f, \mathcal{T}_M)} || P_{(f, \mathcal{X}_{\text{test}})})$ indicates the dissimilarity between $P_{(f, \mathcal{T}_M)}$, the distribution of the measures computed on the synthetic trajectories in \mathcal{T}_M , and $P_{(f, \mathcal{X}_{\text{test}})}$, the distribution of the measures computed on the real trajectories in $\mathcal{X}_{\text{test}}$. The lower $D(P_{(f, \mathcal{T}_M)} || P_{(f, \mathcal{X}_{\text{test}})})$, the more realistic model M is with respect to f and $\mathcal{X}_{\text{test}}$.

Why it is a challenging problem. Trajectory generation requires capturing, simultaneously, the temporal and spatial patterns of human mobility. A realistic generative model should reproduce the temporal statistics observed empirically, including the number and sequence of visited locations together with the time and duration of the visits. In particular, the biggest hurdle consists of the simultaneous description of an individual's routine and sporadic out-of-routine mobility patterns. Regarding spatial patterns, a generative model should reproduce the tendency of individuals to move preferably within short distances [60, 118], the heterogeneity of characteristic distances [60, 118], and the tendency of individuals to split into returners and explorers [121], the fact that human trajectories are routinary and preventable [154], and the fact that individuals visit a number of locations that are constant in time [3]. A complete generative model should capture all spatial and temporal patterns together, a feature that is far from the existing models' capacity.

Traditional approaches. There is a vast literature on mechanistic generative models that reproduce simple temporal, spatial, and social patterns of human mobility [6, 70, 85, 119, 175]. For example, in the Exploration and Preferential Return (EPR) model [153], an agent can choose between two competing mechanisms: exploration, during which an agent chooses a new location never visited before, based on a random walk process with a power-law jump-size distribution; and preferential return, in which an agent returns to a previously visited location based on its frequency. Several studies subsequently improved the EPR model by adding increasingly sophisticated spatial or social mechanisms [3, 7, 121, 169]. EPR and its extensions focus mainly on the spatial aspects of human mobility, implementing unrealistic temporal mechanisms. Two refined models, TimeGeo [79] and DITRAS [119], improve the temporal mechanisms of EPR-like models integrating a Markov chain that captures the circadian propensity to travel and out-of-routine trips. Although mechanistic models have the advantage of being interpretable by design, their realism is limited because of the simplicity of the implemented mechanisms. For this reason, the literature is moving recently to generative mobility models based on DL.

DL approaches. In their vision paper, Liu et al. [103] propose the trajGANs framework to address the potential and challenges of using GANs for trajectory generation. Similar to a typical GAN [62], a trajGAN consists of a generator G , which accepts a random vector z and generates a dense representation of synthetic trajectory samples, and a discriminator D , which classifies an input trajectory sample into “real” or “fake”. Liu et al. [103] suggest the use of Recurrent Neural Networks (RNNs) to create dense representations of trajectories and transform between trajectories and distributional representations.

Ouyang et al. [115] represent a trajectory as a sequence of stays, each with a geographic location, start time and duration. Specifically, a trajectory is an $n_1 \times n_2 \times k$ matrix, where $n_1 \times n_2$ is the size of a squared tessellation, and k is the maximum number of stay repetitions for each location (set in the experiments to $k = 4$). A Wasserstein GAN [68], is used to train a trajectory generator. Both the generator and the discriminator are based on a CNN. The experiments are conducted on the MDC dataset [96] using a 64×64 squared tessellation on the city of Lausanne, Switzerland. The similarity between synthetic and real trajectories is evaluated using the JS divergence on the popularity $p(r)$ and temporal popularity $p(r, t)$ of locations, the staying patterns $p(r, d)$, the semantic importance $p_{d_{total}}(r)$, the semantic distance, and G-rank.

Song et al. [155] use a CNN with four layers within a GAN framework to generate trajectories represented as 512×512 matrices. In a data convolution process, the input 512×512 matrices are resized into a 32×32 matrix. The experiments, given the small size of the available (private) mobile phone datasets, include synthetic ones obtained by randomly shuffling the real trajectories. In a deconvolution process, the GAN’s output (a 32×32 matrix) is resized back to a 512×512 matrix using the nearest neighbor function. No quantitative evaluation of the model’s realism is provided.

Huang et al. [72] present SVAE (Sequential Variational Autoencoder), a generative model based on a combination of a Variational Autoencoder (VAE) and an LSTM, combining the ability of VAEs to construct a latent space that captures salient features of the training data with the ability of LSTMs to process sequential data. In a data processing phase, they force the input trajectories to have fixed timestamps, and in the experiments they evaluate the realism of SVAE through the Mean Distance Error (MDE) between each step of real and synthetic trajectory pairs, finding that the reconstruction error of SVAE is smaller than 800 meters.

Kulkarni et al. [94] benchmark the performance of RNNs, SeqGAN [196], RGAN [45] and nonparametric copulas to generate synthetic trajectories. They compare the generated trajectories with real ones extracted from the MDC dataset [96] based on geographic and semantic similarity, statistical similarity, long-range dependencies and privacy tests. They find that copulas have an advantage over all other methods in terms of both model performance and computational time.

MoveSim [48] is a model-free GAN framework that integrates the domain knowledge of human mobility regularity. The generator consists of a self-attention based sequential model to capture the temporal transitions in human mobility. The discriminator consists of a mobility regularity-aware loss to distinguish the generated trajectory from a fake one. The mobility regularities of spatial continuity and temporal periodicity are used to pre-train the generator and discriminator to accelerate the learning procedure. They conduct experiments on a private mobile phone dataset, using the base station as the spatial unit, and on GeoLife [208], projecting GPS coordinates into the grids containing up to 3 digits after the decimal point. As for the temporal granularity, they set the basic time slot of a trajectory as half an hour of the day. The realism of MoveSim is evaluated based on the distribution of distances, radius of gyration, number of locations visited daily, G-rank, and I-rank using the JS divergence with respect to real trajectories.

Yin et al. [194] use a GAN-based framework to generate density distributions rather than trajectories, i.e., the number of users in each location at each time slot. Both the generator and the discriminator are implemented with FCs. Experiments are conducted on a dataset extracted from MoMo (spatial resolution 2km, time slots of 30 minutes) and on the dataset of taxis in San Francisco (squared tessellation of $50\text{km} \times 50\text{km}$, time slots of two

minutes) [127]. The proposed model evaluated in terms of reconstruction error and utility loss outperforms the differential privacy approach in data utility and attack error.

5 CONCLUSIONS

In this survey, we proposed our perspective on DL approaches to next-location prediction, crowd flow prediction, and trajectory generation. In particular, we provide the reader with an extensive discussion and description of all the key components needed to design, train, and evaluate the models. First, we discuss the main mobility data sources and list a set of public datasets that may be used to train and test the solutions to the problems mentioned above. Second, we introduce the deep learning components used in the state-of-the-art models to give the readers an overview of how these components work and may be combined. Finally, we describe the most relevant DL solutions to the three mobility tasks. As an additional contribution to the community, we created a GitHub repository (bit.ly/DL4HM) where researchers can contribute to maintaining the list of datasets and relevant papers always up-to-date. Our overview of the state of the art of DL models for human mobility reveals that existing solutions suffer from several limitations, and many relevant aspects need to be addressed in the future. In particular, we identify the following open challenges.

Geographic Transferability. Although DL models can capture complex mobility patterns automatically, they strictly depend on the data used for training and may not be *geographically transferable*, i.e., one model trained on a specific region can be used to predict locations or crowd flows or to generate synthetic trajectories on a distinct, non-overlapping region. Geographic transferability can be crucial in situations where there is a scarcity or even absence of mobility data for a region, and it poses several challenges related, for example, to the design of a suitable encoder of the mobility trajectories or flows. As a first tentative in this direction, RegionTrans [176] provides insights on how transferability can be tackled for crowd flow prediction. Still, more work is needed to address this open challenge.

Explainability. DL models are by nature *opaque*, i.e., they are black-boxes from which it is hard to reconstruct the reasoning that led to the generation of a trajectory or the prediction of a location or flow. Nonetheless, explainability is crucial for gaining a deeper understanding of mobility patterns and highlighting the presence of biases in the model's reasoning. It is important to develop mobility-related explanations that provide examples and counter-examples to validate trajectories and crowd flows from different perspectives. While models rely on many features, either external ones (e.g., weather data, POIs) or spatio-temporal ones, it is not clear what the role of each feature is to the model's prediction or generation. Designing explainable DL models for human mobility is essential to gain knowledge that can be useful for possible users, such as policymakers and urban planners.

Privacy. DL models raise privacy issues both in the training and the prediction or generation phase. For example, in trajectory generation, evaluating the risk of re-identifying a real user from synthetic trajectories is crucial, especially when there is a scarcity of data to train the models. A synthetic trajectory may resemble a real one and a malicious adversary may use this information for re-identification. In the training phase, the risk of leaking private data is high regardless of the mobility task, as the portions of information used cannot be controlled directly. The extent training trajectories or crowd flows can be perturbed without degrading the realism of the generative models and the accuracy of predictive ones is an aspect that is barely investigated in the literature.

Tunability. Meaningful predictions and simulations require models that can be controlled along relevant mobility dimensions, such as geographic space, time granularity, presence of mobility restrictions or other events that may alter mobility, predictability of trajectories or crowd flows, and more. Current DL models have a limited degree of tunability, which limits their usability in practice. For example, it is not clear to what extent the models' realism or accuracy depends on the size or shape of the spatial tessellation, which may vary according to the

user's needs. For example, suppose the decision-maker is interested in identifying the most active areas of a city in terms of daily mobility. In that case, the usage of administrative tiles may provide more interpretable results. In contrast, if they want to understand how the transportation and road networks affect and are affected by big events in a city, the usage of fine-grained grid-like tessellations may be helpful.

Interaction Dimension. Next-location predictors and trajectory generators assume the independence of the individuals' mobility, even though social purposes or collective needs can explain a significant portion of human movements. People's movements are not entirely independent of each other and they can lead to situations like traffic jams, accidents, or massive commuting patterns. Models that can include these aspects need to be designed to capture human mobility's complexity more comprehensively.

ACKNOWLEDGMENTS

Luca Pappalardo has been partially supported by EU H2020 SoBigData++ grant agreement #871042.

REFERENCES

- [1] Mohammed N Ahmed, Gianni Barlacchi, Stefano Braghin, Francesco Calabrese, Michele Ferretti, Vincent PA Lonij, Rahul Nair, Rana Novack, Jurij Paraszczak, and Andeep S Toor. 2016. A Multi-Scale Approach to Data-Driven Mass Migration Analysis.. In *SoGood@ ECML-PKDD*.
- [2] Yi Ai, Zongping Li, Mi Gan, Yunpeng Zhang, Daben Yu, Wei Chen, and Yanni Ju. 2019. A deep learning approach on short-term spatiotemporal distribution forecasting of dockless bike-sharing system. *Neural Computing and Applications* 31, 5 (2019), 1665–1677.
- [3] Laura Alessandretti, Piotr Sapiezynski, Vedran Sekara, Sune Lehmann, and Andrea Baronchelli. 2018. Evidence for a conserved quantity in human mobility. *Nature Human Behaviour* 2, 7 (2018), 485–491.
- [4] Gennady Andrienko, Natalia Andrienko, Chiara Boldrini, Guido Caldarelli, Paolo Cintia, Stefano Cresci, Angelo Facchini, Fosca Giannotti, Aristides Gionis, Riccardo Guidotti, Michael Mathioudakis, Cristina Ioana Muntean, Luca Pappalardo, Dino Pedreschi, Evangelos Pournaras, Francesca Pratesi, Maurizio Tesconi, and Roberto Trasarti. 2020. (So) Big Data and the transformation of the city. *International Journal of Data Science and Analytics* (2020).
- [5] Daniel Ashbrook and Thad Starner. 2002. Learning significant locations and predicting user movement with GPS. In *Proceedings. Sixth International Symposium on Wearable Computers.*, 101–108.
- [6] Hugo Barbosa, Marc Barthelemy, Gourab Ghoshal, Charlotte R James, Maxime Lenormand, Thomas Louail, Ronaldo Menezes, José J Ramasco, Filippo Simini, and Marcello Tomasini. 2018. Human mobility: Models and applications. *Physics Reports* 734 (2018), 1–74.
- [7] Hugo Barbosa, Fernando B de Lima-Neto, Alexandre Evsukoff, and Ronaldo Menezes. 2015. The effect of recency to human mobility. *EPJ Data Science* 4 (2015), 1–14.
- [8] Gianni Barlacchi, Marco De Nadai, Roberto Larcher, Antonio Casella, Cristiana Chitic, Giovanni Torrisi, Fabrizio Antonelli, Alessandro Vespignani, Alex Pentland, and Bruno Lepri. 2015. A multi-source dataset of urban life in the city of Milan and the Province of Trentino. *Scientific data* 2 (2015), 150055.
- [9] Gianni Barlacchi, Christos Perentis, Abhinav Mehrotra, Mirco Musolesi, and Bruno Lepri. 2017. Are you getting sick? Predicting influenza-like symptoms using human mobility behaviors. *EPJ Data Science* 6, 1 (2017), 27.
- [10] Gianni Barlacchi, Alberto Rossi, Bruno Lepri, and Alessandro Moschitti. 2017. Structural semantic models for automatic analysis of urban areas. In *Joint European Conference on Machine Learning and Knowledge Discovery in Databases*. Springer, 279–291.
- [11] Armando Bazzani, Bruno Giorgini, Sandro Rambaldi, Riccardo Gallotti, and Luca Giovannini. 2010. Statistical laws in urban mobility from microscopic GPS data in the area of Florence. *Journal of Statistical Mechanics: Theory and Experiment* 2010, 05 (2010), P05001.
- [12] Citi Bike. 2013. *Citi Bike System Data - NYC*. <https://www.citibikenyc.com/system-data>
- [13] Capital Bikeshare. 2011. *Capital Bikeshare - Washington DC*. <https://www.capitalbikeshare.com/system-data>
- [14] V. Bindschaedler and R. Shokri. 2016. Synthesizing Plausible Privacy-Preserving Location Traces. In *2016 IEEE Symposium on Security and Privacy (SP)*. 546–563.
- [15] Justine I. Blanford, Zhuojie Huang, Alexander Savelyev, and Alan M. MacEachren. 2015. Geo-Located Tweets. Enhancing Mobility Maps and Capturing Cross-Border Movement. *PLOS ONE* 10, 6 (2015), 1–16.
- [16] Vincent D. Blondel, Adeline Decuyper, and Gautier Krings. 2015. A survey of results on mobile phone datasets analysis. *EPJ Data Science* 4, 1 (2015), 10.
- [17] George EP Box, Gwilym M Jenkins, Gregory C Reinsel, and Greta M Ljung. 2015. *Time series analysis: forecasting and control*. John Wiley & Sons.

- [18] Lorenzo Bracciale, Marco Bonola, Pierpaolo Loreti, Giuseppe Bianchi, Raul Amici, and Antonello Rabuffi. 2014. CRAWDAD dataset roma/taxi (v. 2014-07-17).
- [19] Dirk Brockmann, Lars Hufnagel, and Theo Geisel. 2006. The scaling laws of human travel. *Nature* 439, 7075 (2006), 462–465.
- [20] Ingrid Burbey and Thomas L Martin. 2012. A survey on predicting personal mobility. *International Journal of Pervasive Computing and Communications* (2012).
- [21] F. Calabrese, G. Di Lorenzo, L. Liu, and C. Ratti. 2011. Estimating Origin-Destination Flows Using Mobile Phone Location Data. *IEEE Pervasive Computing* (2011), 36–44.
- [22] Francesco Calabrese, Giusy Di Lorenzo, and Carlo Ratti. 2010. Human mobility prediction based on individual and collective geographical preferences. In *13th international IEEE conference on intelligent transportation systems*. 312–317.
- [23] Luca Canzian and Mirco Musolesi. 2015. Trajectories of depression: unobtrusive monitoring of depressive states by means of smartphone mobility traces analysis. In *Proceedings of the 2015 ACM International Joint Conference on Pervasive and Ubiquitous Computing*. 1293–1304.
- [24] Justin David Carlson. 2010. *Mapping Large, Urban Environments with GPS-Aided SLAM*. Ph.D. Dissertation. Carnegie Mellon University.
- [25] Shwu-Jing Chang, Gong-Ying Hsu, Jia-Ao Yang, Kuan-Ning Chen, Yung-Fang Chiu, and Fu-Tong Chang. 2010. Vessel traffic analysis for maritime Intelligent Transportation System. In *2010 IEEE 71st Vehicular Technology Conference*. IEEE, 1–4.
- [26] Guangshuo Chen, Aline Carneiro Viana, Marco Fiore, and Carlos Sarraute. 2019. Complete trajectory reconstruction from sparse mobile phone data. *EPJ Data Science* 8, 1 (2019), 30.
- [27] J. Chen, Z. Xiao, D. Wang, W. Long, and V. Havyarimana. 2019. Stay of Interest: A Dynamic Spatiotemporal Stay Behavior Perception Method for Private Car Users. In *2019 IEEE 21st International Conference on High Performance Computing and Communications*. 1526–1532.
- [28] Yile Chen, Cheng Long, Gao Cong, and Chenliang Li. 2020. Context-aware Deep Model for Joint Mobility and Time Prediction. In *Proceedings of the 13th International Conference on Web Search and Data Mining*. 106–114.
- [29] Eunjoon Cho, Seth A Myers, and Jure Leskovec. 2011. Friendship and mobility: user movement in location-based social networks. In *Proceedings of the 17th ACM SIGKDD international conference on Knowledge discovery and data mining*. 1082–1090.
- [30] Kyunghyun Cho, Bart van Merriënboer, Caglar Gulcehre, Dzmitry Bahdanau, Fethi Bougares, Holger Schwenk, and Yoshua Bengio. 2014. Learning Phrase Representations using RNN Encoder–Decoder for Statistical Machine Translation. In *Proceedings of the 2014 Conference on Empirical Methods in Natural Language Processing (EMNLP)*. Association for Computational Linguistics, 1724–1734.
- [31] Kyunghyun Cho, Bart Van Merriënboer, Caglar Gulcehre, Dzmitry Bahdanau, Fethi Bougares, Holger Schwenk, and Yoshua Bengio. 2014. Learning phrase representations using RNN encoder-decoder for statistical machine translation. *arXiv preprint arXiv:1406.1078* (2014).
- [32] Edward Choi, Mohammad Taha Bahadori, Jimeng Sun, Joshua Kulas, Andy Schuetz, and Walter Stewart. 2016. Retain: An interpretable predictive model for healthcare using reverse time attention mechanism. In *Advances in Neural Information Processing Systems*. 3504–3512.
- [33] Jan K Chorowski, Dzmitry Bahdanau, Dmitriy Serdyuk, Kyunghyun Cho, and Yoshua Bengio. 2015. Attention-based models for speech recognition. In *Advances in neural information processing systems*. 577–585.
- [34] Balázs Cs Csáji, Arnaud Browet, Vincent A Traag, Jean-Charles Delvenne, Etienne Huens, Paul Van Dooren, Zbigniew Smoreda, and Vincent D Blondel. 2013. Exploring the mobility of mobile phone users. *Physica A: statistical mechanics and its applications* 392, 6 (2013), 1459–1473.
- [35] Yilan Cui, Xing Xie, and Yi Liu. 2018. Social media and mobility landscape: Uncovering spatial patterns of urban human mobility with multi source data. *Frontiers of Environmental Science & Engineering* 12, 5 (2018), 7.
- [36] Alexandre De Brébisson, Étienne Simon, Alex Auvolet, Pascal Vincent, and Yoshua Bengio. 2015. Artificial neural networks applied to taxi destination prediction. In *Proceedings of the 2015th International Conference on ECML PKDD Discovery Challenge*. 40–51.
- [37] Yves-Alexandre de Montjoye, Sébastien Gambs, Vincent Blondel, Geoffrey Canright, Nicolas de Cordes, Sébastien Deletaille, Kenth Engø-Monsen, Manuel Garcia-Herranz, Jake Kendall, Cameron Kerry, Gautier Krings, Emmanuel Letouzé, Miguel Luengo-Oroz, Nuria Oliver, Luc Rocher, Alex Rutherford, Zbigniew Smoreda, Jessica Steele, Erik Wetter, Alex “Sandy” Pentland, and Linus Bengtsson. 2018. On the privacy-conscious use of mobile phone data. *Scientific Data* 5, 1 (2018), 180286.
- [38] Mark S Dougherty and Mark R Cobbett. 1997. Short-term inter-urban traffic forecasts using neural networks. *International journal of forecasting* 13, 1 (1997), 21–31.
- [39] Bowen Du, Hao Peng, Senzhang Wang, Md Zakirul Alam Bhuiyan, Lihong Wang, Qiran Gong, Lin Liu, and Jing Li. 2019. Deep irregular convolutional residual LSTM for urban traffic passenger flows prediction. *IEEE Transactions on Intelligent Transportation Systems* 21, 3 (2019), 972–985.
- [40] Zhanwei Du, Yongjian Yang, Zeynep Ertem, Chao Gao, Liping Huang, Qiuyang Huang, and Yuan Bai. 2019. Inter-urban mobility via cellular position tracking in the southeast Songliao Basin, Northeast China. *Scientific data* 6, 1 (2019), 1–6.
- [41] Zhanwei Du, Yongjian Yang, Chao Gao, Liping Huang, Qiuyang Huang, and Yuan Bai. 2018. The temporal network of mobile phone users in Changchun Municipality, Northeast China. *Scientific data* 5, 1 (2018), 1–7.

- [42] Nathan Eagle and Alex Sandy Pentland. 2009. Eigenbehaviors: identifying structure in routine. *Behavioral Ecology and Sociobiology* 63, 11 (2009), 1689–1689.
- [43] Patrick Ebel, Ibrahim Emre Göl, Christoph Lingenfelder, and Andreas Vogelsang. 2020. Destination Prediction Based on Partial Trajectory Data. *arXiv preprint arXiv:2004.07473* (2020).
- [44] Zeinab Ebrahimpour, Wanggen Wan, Ofelia Cervantes, Tianhang Luo, and Hidayat Ullah. 2019. Comparison of main approaches for extracting behavior features from crowd flow analysis. *ISPRS International Journal of Geo-Information* 8, 10 (2019), 440.
- [45] Cristóbal Esteban, Stephanie L Hyland, and Gunnar Rättsch. 2017. Real-valued (medical) time series generation with recurrent conditional gans. *arXiv preprint arXiv:1706.02633* (2017).
- [46] Clement Farabet, Camille Couprie, Laurent Najman, and Yann LeCun. 2013. Learning Hierarchical Features for Scene Labeling. *IEEE Trans. Pattern Anal. Mach. Intell.* 35, 8 (2013), 1915–1929.
- [47] Jie Feng, Yong Li, Chao Zhang, Funing Sun, Fanchao Meng, Ang Guo, and Depeng Jin. 2018. Deepmove: Predicting human mobility with attentional recurrent networks. In *Proceedings of the 2018 world wide web conference*. 1459–1468.
- [48] Jie Feng, Zeyu Yang, Fengli Xu, Haisu Yu, Mudan Wang, and Yong Li. 2020. Learning to Simulate Human Mobility. In *Proceedings of the 26th ACM SIGKDD International Conference on Knowledge Discovery & Data Mining (Virtual Event, CA, USA) (KDD '20)*. Association for Computing Machinery, New York, NY, USA, 3426–3433. <https://doi.org/10.1145/3394486.3412862>
- [49] Yunhe Feng and Wenjun Zhou. 2020. Is Working From Home The New Norm? An Observational Study Based on a Large Geo-tagged COVID-19 Twitter Dataset. *arXiv:cs.SI/2006.08581*
- [50] Z. Feng and Y. Zhu. 2016. A Survey on Trajectory Data Mining: Techniques and Applications. *IEEE Access* 4 (2016), 2056–2067.
- [51] V. Fernandez Arguedas, G. Pallotta, and M. Vespe. 2018. Maritime Traffic Networks: From Historical Positioning Data to Unsupervised Maritime Traffic Monitoring. *IEEE Transactions on Intelligent Transportation Systems* 19, 3 (2018), 722–732.
- [52] Michele Ferretti, Gianni Barlacchi, Luca Pappalardo, Lorenzo Lucchini, and Bruno Lepri. 2018. Weak nodes detection in urban transport systems: Planning for resilience in Singapore. In *2018 IEEE 5th international conference on data science and advanced analytics (DSAA)*. IEEE, 472–480.
- [53] Marco Fiore, Panagiota Katsikouli, Elli Zavou, Mathieu Cunche, Françoise Fessant, Dominique Le Hello, Ulrich Matchi Aivodji, Baptiste Olivier, Tony Quertier, and Razvan Stanica. 2019. Privacy in trajectory micro-data publishing : a survey. *arXiv: Cryptography and Security* (2019).
- [54] LIVIO Florio and LORENZO Mussone. 1996. Neural-network models for classification and forecasting of freeway traffic flow stability. *Control Engineering Practice* 4, 2 (1996), 153–164.
- [55] Riccardo Gallotti, Armando Bazzani, Mirko Degli Esposti, and Sandro Rambaldi. 2013. Entropic measures of individual mobility patterns. *Journal of Statistical Mechanics: Theory and Experiment* 2013, 10 (2013), P10022.
- [56] Riccardo Gallotti, Armando Bazzani, Sandro Rambaldi, and Marc Barthelemy. 2016. A stochastic model of randomly accelerated walkers for human mobility. *Nature Communications* 7, 1 (2016), 12600.
- [57] Sébastien Gams, Marc-Olivier Killijian, and Miguel Núñez del Prado Cortez. 2010. Show me how you move and I will tell you who you are. In *Proceedings of the 3rd ACM SIGSPATIAL International Workshop on Security and Privacy in GIS and LBS*. 34–41.
- [58] Sébastien Gams, Marc-Olivier Killijian, and Miguel Núñez del Prado Cortez. 2012. Next place prediction using mobility markov chains. In *Proceedings of the First Workshop on Measurement, Privacy, and Mobility*. 1–6.
- [59] Qiang Gao, Fan Zhou, Goce Trajcevski, Kunpeng Zhang, Ting Zhong, and Fengli Zhang. 2019. Predicting human mobility via variational attention. In *The World Wide Web Conference*. 2750–2756.
- [60] Marta C Gonzalez, Cesar A Hidalgo, and Albert-Laszlo Barabasi. 2008. Understanding individual human mobility patterns. *nature* 453, 7196 (2008), 779–782.
- [61] Ian Goodfellow, Yoshua Bengio, Aaron Courville, and Yoshua Bengio. 2016. *Deep learning*. Vol. 1. MIT press Cambridge.
- [62] Ian J. Goodfellow, Jean Pouget-Abadie, Mehdi Mirza, Bing Xu, David Warde-Farley, Sherjil Ozair, Aaron Courville, and Yoshua Bengio. 2014. Generative Adversarial Nets. In *Proceedings of the 27th International Conference on Neural Information Processing Systems*. 2672–2680.
- [63] Alex Graves, Navdeep Jaitly, and Abdel-rahman Mohamed. 2013. Hybrid speech recognition with deep bidirectional LSTM. In *2013 IEEE workshop on automatic speech recognition and understanding*. IEEE, 273–278.
- [64] Alex Graves and Jürgen Schmidhuber. 2005. Framewise phoneme classification with bidirectional LSTM and other neural network architectures. *Neural networks* 18, 5-6 (2005), 602–610.
- [65] Clark L Gray and Valerie Mueller. 2012. Natural disasters and population mobility in Bangladesh. *Proceedings of the National Academy of Sciences* 109, 16 (2012), 6000–6005.
- [66] Valerio Grossi, Beatrice Rapisarda, Fosca Giannotti, and Dino Pedreschi. 2018. Data science at SoBigData: the European research infrastructure for social mining and big data analytics. *International Journal of Data Science and Analytics* 6, 3 (2018), 205–216.
- [67] Aditya Grover and Jure Leskovec. 2016. Node2vec: Scalable Feature Learning for Networks. In *Proceedings of the 22nd ACM SIGKDD International Conference on Knowledge Discovery and Data Mining*. Association for Computing Machinery, 855–864.

- [68] Ishaan Gulrajani, Faruk Ahmed, Martin Arjovsky, Vincent Dumoulin, and Aaron Courville. 2017. Improved Training of Wasserstein GANs. In *Proceedings of the 31st International Conference on Neural Information Processing Systems*. 5769–5779.
- [69] Kaiming He, Xiangyu Zhang, Shaoqing Ren, and Jian Sun. 2016. Deep residual learning for image recognition. In *Proceedings of the IEEE conference on computer vision and pattern recognition*. 770–778.
- [70] Andrea Hess, Karin Anna Hummel, Wilfried N Gansterer, and Günter Haring. 2015. Data-driven human mobility modeling: a survey and engineering guidance for mobile networking. *ACM Computing Surveys (CSUR)* 48, 3 (2015), 1–39.
- [71] Sepp Hochreiter and Jürgen Schmidhuber. 1997. Long short-term memory. *Neural computation* 9, 8 (1997), 1735–1780.
- [72] D. Huang, X. Song, Z. Fan, R. Jiang, R. Shibasaki, Y. Zhang, H. Wang, and Y. Kato. 2019. A Variational Autoencoder Based Generative Model of Urban Human Mobility. In *2019 IEEE Conference on Multimedia Information Processing and Retrieval (MIPR)*. 425–430.
- [73] G. Huang, Z. Liu, L. Van Der Maaten, and K. Q. Weinberger. 2017. Densely Connected Convolutional Networks. In *2017 IEEE Conference on Computer Vision and Pattern Recognition (CVPR)*. 2261–2269.
- [74] D H HUBEL and T N WIESEL. 1959. Receptive fields of single neurones in the cat’s striate cortex. *The Journal of physiology* 148, 3 (1959), 574–591.
- [75] D. H. Hubel and T. N. Wiesel. 1962. Receptive fields, binocular interaction and functional architecture in the cat’s visual cortex. *The Journal of Physiology* 160, 1 (1962), 106–154.
- [76] Kasthuri Jayarajah, Andrew Tan, and Archan Misra. 2018. Understanding the Interdependency of Land Use and Mobility for Urban Planning. In *Proceedings of the 2018 ACM International Joint Conference and 2018 International Symposium on Pervasive and Ubiquitous Computing and Wearable Computers*. Association for Computing Machinery, 1079–1087.
- [77] Renhe Jiang, Xuan Song, Zipei Fan, Tianqi Xia, Quanjun Chen, Satoshi Miyazawa, and Ryosuke Shibasaki. 2018. Deepurbanmomentum: An online deep-learning system for short-term urban mobility prediction. In *Thirty-Second AAAI Conference on Artificial Intelligence*.
- [78] Shan Jiang, Gaston A. Fiore, Yingxiang Yang, Joseph Ferreira, Emilio Frazzoli, and Marta C. González. 2013. A Review of Urban Computing for Mobile Phone Traces: Current Methods, Challenges and Opportunities. In *Proceedings of the 2nd ACM SIGKDD International Workshop on Urban Computing*.
- [79] Shan Jiang, Yingxiang Yang, Siddharth Gupta, Daniele Veneziano, Shounak Athavale, and Marta C. Gonzalez. 2016. The TimeGeo modeling framework for urban mobility without travel surveys. *Proceedings of the National Academy of Sciences* 113 (2016), 201524261.
- [80] Wenwei Jin, Youfang Lin, Zhihao Wu, and Huaiyu Wan. 2018. Spatio-Temporal Recurrent Convolutional Networks for Citywide Short-Term Crowd Flows Prediction.
- [81] Ma Jun and Meng Ying. 2008. Research of traffic flow forecasting based on neural network. In *2008 Second International Symposium on Intelligent Information Technology Application*, Vol. 2. IEEE, 104–108.
- [82] Raja Jurdak, Kun Zhao, Jiajun Liu, Maurice AbouJaoude, Mark Cameron, and David Newth. 2015. Understanding Human Mobility from Twitter. *PLOS ONE* 10, 7 (2015), 1–16.
- [83] Yiannis Kamarianakis and Poulicos Prastacos. 2003. Forecasting traffic flow conditions in an urban network: Comparison of multivariate and univariate approaches. *Transportation Research Record* 1857, 1 (2003), 74–84.
- [84] Yiannis Kamarianakis and Poulicos Prastacos. 2005. Space-time modeling of traffic flow. *Computers & Geosciences* 31, 2 (2005), 119–133.
- [85] Dmytro Karamshuk, Chiara Boldrini, Marco Conti, and Andrea Passarella. 2011. Human mobility models for opportunistic networks. *IEEE Communications Magazine* 49, 12 (2011), 157–165.
- [86] L. Khaidem, M. Luca, F. Yang, A. Anand, B. Lepri, and W. Dong. 2020. Optimizing Transportation Dynamics at a City-Scale Using a Reinforcement Learning Framework. *IEEE Access* 8 (2020), 171528–171541.
- [87] Asifullah Khan, Anabia Sohail, Umme Zahoor, and Aqsa Saeed Qureshi. 2020. A survey of the recent architectures of deep convolutional neural networks. *Artificial Intelligence Review* (2020).
- [88] Niko Kiukkonen, Jan Blom, Olivier Dousse, Daniel Gatica-Perez, and Juha Laurila. 2010. Towards rich mobile phone datasets: Lausanne data collection campaign. *Proc. ICPS, Berlin* 68 (2010).
- [89] J. F. Kolen and S. C. Kremer. 2001. *Gradient Flow in Recurrent Nets: The Difficulty of Learning Long-Term Dependencies*. 237–243.
- [90] Dejiang Kong and Fei Wu. 2018. HST-LSTM: A Hierarchical Spatial-Temporal Long-Short Term Memory Network for Location Prediction. In *IJCAL* 2341–2347.
- [91] Vartika Koolwal and Krishna Kumar Mohbey. 2020. A comprehensive survey on trajectory-based location prediction. *Iran Journal of Computer Science* 3, 2 (2020), 65–91.
- [92] Moritz UG Kraemer, Chia-Hung Yang, Bernardo Gutierrez, Chieh-Hsi Wu, Brennan Klein, David M Pigott, Louis Du Plessis, Nuno R Faria, Ruoran Li, William P Hanage, et al. 2020. The effect of human mobility and control measures on the COVID-19 epidemic in China. *Science* 368, 6490 (2020), 493–497.
- [93] Alex Krizhevsky, Ilya Sutskever, and Geoffrey E Hinton. 2012. ImageNet Classification with Deep Convolutional Neural Networks. In *Advances in Neural Information Processing Systems* 25, F. Pereira, C. J. C. Burges, L. Bottou, and K. Q. Weinberger (Eds.). Curran Associates, Inc., 1097–1105.
- [94] Vaibhav Kulkarni, Natasa Tagasovska, Thibault Vatter, and Benoit Garbinato. 2018. Generative models for simulating mobility trajectories. *arXiv preprint arXiv:1811.12801* (2018).

- [95] Shengjie Lai, Andrea Farnham, Nick W Ruktanonchai, and Andrew J Tatem. 2019. Measuring mobility, disease connectivity and individual risk: a review of using mobile phone data and Health for travel medicine. *Journal of travel medicine* 26, 3 (2019).
- [96] Juha K Laurila, Daniel Gatica-Perez, Imad Aad, Olivier Borneo, Trinh-Minh-Tri Do, Olivier Dousse, Julien Eberle, Markus Miettinen, et al. 2012. *The mobile data challenge: Big data for mobile computing research*. Technical Report.
- [97] Sangsoo Lee and Daniel B Fambro. 1999. Application of subset autoregressive integrated moving average model for short-term freeway traffic volume forecasting. *Transportation Research Record* 1678, 1 (1999), 179–188.
- [98] Wei Li, Wei Tao, Junyang Qiu, Xin Liu, Xingyu Zhou, and Zhisong Pan. 2019. Densely Connected Convolutional Networks With Attention LSTM for Crowd Flows Prediction. *IEEE Access* 7 (2019), 140488–140498.
- [99] Yuan Liao, Sonia Yeh, and Gustavo S Jeuken. 2019. From individual to collective behaviours: exploring population heterogeneity of human mobility based on social media data. *EPJ Data Science* 8, 1 (2019), 34.
- [100] Ziqian Lin, Jie Feng, Ziyang Lu, Yong Li, and Depeng Jin. 2019. Deepstn+: Context-aware spatial-temporal neural network for crowd flow prediction in metropolis. In *Proceedings of the AAAI Conference on Artificial Intelligence*, Vol. 33. 1020–1027.
- [101] Lingbo Liu, Jiajie Zhen, Guanbin Li, Geng Zhan, Zhaocheng He, Bowen Du, and Liang Lin. 2020. Dynamic Spatial-Temporal Representation Learning for Traffic Flow Prediction. *IEEE Transactions on Intelligent Transportation Systems* (2020).
- [102] Qiang Liu, Shu Wu, Liang Wang, and Tieniu Tan. 2016. Predicting the next location: A recurrent model with spatial and temporal contexts. In *Thirtieth AAAI conference on artificial intelligence*.
- [103] Xi Liu, Hanzhou Chen, and Clio Andris. 2018. trajGANs: Using generative adversarial networks for geo-privacy protection of trajectory data (Vision paper). In *Location Privacy and Security Workshop*. 1–7.
- [104] Jianming Lv, Qing Li, Qinghui Sun, and Xintong Wang. 2018. T-CONV: A convolutional neural network for multi-scale taxi trajectory prediction. In *2018 IEEE international conference on big data and smart computing (bigcomp)*. 82–89.
- [105] Jean Damascène Mazimpaka and Sabine Timpf. 2016. Trajectory data mining: A review of methods and applications. *Journal of Spatial Information Science* 2016, 13 (2016), 61–99.
- [106] D. J. Mir, S. Isaacman, R. Cáceres, M. Martonosi, and R. N. Wright. 2013. DP-WHERE: Differentially private modeling of human mobility. In *2013 IEEE International Conference on Big Data*. 580–588.
- [107] Anna Monreale, Fabio Pinelli, Roberto Trasarti, and Fosca Giannotti. 2009. Wherenext: a location predictor on trajectory pattern mining. In *Proceedings of the 15th ACM SIGKDD international conference on Knowledge discovery and data mining*. 637–646.
- [108] CK Moorthy and BG Ratcliffe. 1988. Short term traffic forecasting using time series methods. *Transportation planning and technology* 12, 1 (1988), 45–56.
- [109] Luis Moreira-Matias, Joao Gama, Michel Ferreira, Joao Mendes-Moreira, and Luis Damas. 2013. Predicting taxi-passenger demand using streaming data. *IEEE Transactions on Intelligent Transportation Systems* 14, 3 (2013), 1393–1402.
- [110] Anastasios Noulas, Salvatore Scellato, Renaud Lambiotte, Massimiliano Pontil, and Cecilia Mascolo. 2012. A Tale of Many Cities: Universal Patterns in Human Urban Mobility. *PLOS ONE* 7, 5 (2012), 1–10.
- [111] MM Nyhan, I Kloog, R Britter, C Ratti, and P Koutrakis. 2019. Quantifying population exposure to air pollution using individual mobility patterns inferred from mobile phone data. *Journal of exposure science & environmental epidemiology* 29, 2 (2019), 238.
- [112] Umair Qazi; Muhammad Imran; Ferda Ofli. 2020. GeoCoV19: A Dataset of Hundreds of Millions of Multilingual COVID-19 Tweets with Location Information. <https://doi.org/10.21227/et8d-w881>
- [113] Nuria Oliver, Bruno Lepri, Harald Sterly, Renaud Lambiotte, Sébastien Deletaille, Marco De Nadai, Emmanuel Letouzé, Albert Ali Salah, Richard Benjamins, Ciro Cattuto, et al. 2020. Mobile phone data for informing public health actions across the COVID-19 pandemic life cycle.
- [114] OpenStreetMap. 2013. *OpenStreetMap Bulk GPX track data*. <https://blog.osmfoundation.org/2013/04/12/bulk-gpx-track-data/>
- [115] Kun Ouyang, Reza Shokri, David S Rosenblum, and Wenzhuo Yang. 2018. A Non-Parametric Generative Model for Human Trajectories.. In *IJCAI*. 3812–3817.
- [116] Luca Pappalardo, Giuliano Cornacchia, Victor Navarro, Loreto Bravo, and Leo Ferres. 2020. A dataset to assess mobility changes in Chile following local quarantines. [arXiv:physics.soc-ph/2011.12162](https://arxiv.org/abs/2011.12162)
- [117] Luca Pappalardo, Leo Ferres, Manuel Sacasa, Ciro Cattuto, and Loreto Bravo. 2020. An individual-level ground truth dataset for home location detection. [arXiv:2010.08814](https://arxiv.org/abs/2010.08814)
- [118] Luca Pappalardo, Salvatore Rinzivillo, Zehui Qu, Dino Pedreschi, and Fosca Giannotti. 2013. Understanding the patterns of car travel. *The European Physical Journal Special Topics* 215, 1 (2013), 61–73.
- [119] Luca Pappalardo and Filippo Simini. 2018. Data-driven generation of spatio-temporal routines in human mobility. *Data Mining and Knowledge Discovery* 32, 3 (2018), 787–829.
- [120] Luca Pappalardo, F Simini, G Barlacchi, and R Pellungrini. 2019. scikit-mobility: A Python library for the analysis, generation and risk assessment of mobility data. *arXiv preprint arXiv:1907.07062* (2019).
- [121] Luca Pappalardo, Filippo Simini, Salvatore Rinzivillo, Dino Pedreschi, Fosca Giannotti, and Albert-László Barabási. 2015. Returners and explorers dichotomy in human mobility. *Nature Communications* 6, 1 (2015), 8166.

- [122] Luca Pappalardo, Maarten Vanhoof, Lorenzo Gabrielli, Zbigniew Smoreda, Dino Pedreschi, and Fosca Giannotti. 2016. An analytical framework to nowcast well-being using mobile phone data. *International Journal of Data Science and Analytics* (2016), 75–92.
- [123] Roberto Pellungrini, Luca Pappalardo, Francesca Pratesi, and Anna Monreale. 2017. A Data Mining Approach to Assess Privacy Risk in Human Mobility Data. *ACM Transactions on Intelligent Systems and Technologies* 9, 3 (2017).
- [124] R. Pellungrini, L. Pappalardo, F. Simini, and A. Monreale. 2020. Modeling Adversarial Behavior Against Mobility Data Privacy. *IEEE Transactions on Intelligent Transportation Systems* (2020), 1–14.
- [125] Emanuele Pepe, Paolo Bajardi, Laetitia Gauvin, Filippo Privitera, Brennan Lake, Ciro Cattuto, and Michele Tizzoni. 2020. COVID-19 outbreak response, a dataset to assess mobility changes in Italy following national lockdown. *Scientific data* 7, 1 (2020), 1–7.
- [126] Christos Perentis, Michele Vescovi, Chiara Leonardi, Corrado Moiso, Mirco Musolesi, Fabio Pianesi, and Bruno Lepri. 2017. Anonymous or Not? Understanding the Factors Affecting Personal Mobile Data Disclosure. *ACM Trans. Internet Technol.* 17, 2 (2017).
- [127] Michal Piorkowski, Natasa Sarafijanovic-Djukic, and Matthias Grossglauser. 2009. CRAWDAD dataset epfl/mobility (v. 2009-02-24).
- [128] Rafael Prieto Curiel, Luca Pappalardo, Lorenzo Gabrielli, and Steven Richard Bishop. 2018. Gravity and scaling laws of city to city migration. *PLOS ONE* 13, 7 (2018), 1–19.
- [129] F. Rebelo, C. Soares, and R. J. F. Rossetti. 2015. TwitterJam: Identification of mobility patterns in urban centers based on tweets. In *2015 IEEE First International Smart Cities Conference (ISC2)*. 1–6.
- [130] Shaoqing Ren, Kaiming He, Ross Girshick, and Jian Sun. 2015. Faster R-CNN: Towards Real-Time Object Detection with Region Proposal Networks. In *Proceedings of the 28th International Conference on Neural Information Processing Systems*. 91–99.
- [131] Yibin Ren, Huanfa Chen, Yong Han, Tao Cheng, Yang Zhang, and Ge Chen. 2020. A hybrid integrated deep learning model for the prediction of citywide spatio-temporal flow volumes. *International Journal of Geographical Information Science* 34, 4 (2020), 802–823.
- [132] Rafael Reuveny. 2007. Climate change-induced migration and violent conflict. *Political geography* 26, 6 (2007), 656–673.
- [133] S. Rinzivillo, L. Gabrielli, M. Nanni, L. Pappalardo, D. Pedreschi, and F. Giannotti. 2014. The purpose of motion: Learning activities from Individual Mobility Networks. In *2014 International Conference on Data Science and Advanced Analytics (DSAA)*. 312–318.
- [134] Maria Riveiro, Giuliana Pallotta, and Michele Vespe. 2018. Maritime anomaly detection: A review. *Wiley Interdisciplinary Reviews: Data Mining and Knowledge Discovery* 8, 5 (2018), e1266.
- [135] Alberto Rossi, Gianni Barlacchi, Monica Bianchini, and Bruno Lepri. 2019. Modelling Taxi Drivers’ Behaviour for the Next Destination Prediction. *IEEE Transactions on Intelligent Transportation Systems* (2019).
- [136] Alessio Rossi, Luca Pappalardo, Paolo Cintia, F. Marcello Iaia, Javier Fernández, and Daniel Medina. 2018. Effective injury forecasting in soccer with GPS training data and machine learning. *PLOS ONE* 13, 7 (2018), 1–15.
- [137] Luca Rossi, Matthew J. Williams, Christopher Stich, and Mirco Musolesi. 2015. Privacy and the City: User Identification and Location Semantics in Location-Based Social Networks. In *Proceedings of the 9th International AAAI Conference on Web and Social Media*.
- [138] N. W. Ruktanonchai, J. R. Floyd, S. Lai, C. W. Ruktanonchai, A. Sadilek, P. Rente-Lourenco, X. Ben, A. Carioli, J. Gwinn, J. E. Steele, O. Prosper, A. Schneider, A. Oplinger, P. Eastham, and A. J. Tatem. 2020. Assessing the impact of coordinated COVID-19 exit strategies across Europe. *Science* 369, 6510 (2020), 1465–1470.
- [139] D. E. Rumelhart, G. E. Hinton, and R. J. Williams. 1986. *Learning Internal Representations by Error Propagation*. MIT Press, 318–362.
- [140] T. Russo, L. D’Andrea, A. Parisi, M. Martinelli, A. Belardinelli, F. Boccoli, I. Cignini, M. Tordoni, and S. Cataudella. 2016. Assessing the fishing footprint using data integrated from different tracking devices: Issues and opportunities. *Ecological Indicators* 69 (2016), 818 – 827.
- [141] BA Sabarish, R Karthi, and T Gireeshkumar. 2015. A survey of location prediction using trajectory mining. In *Artificial Intelligence and Evolutionary Algorithms in Engineering Systems*. Springer, 119–127.
- [142] Christian M. Schneider, Vitaly Belik, Thomas Couronné, Zbigniew Smoreda, and Marta C. González. 2013. Unravelling daily human mobility motifs. *Journal of The Royal Society Interface* 10, 84 (2013), 20130246.
- [143] M. Schuster and K. K. Paliwal. 1997. Bidirectional recurrent neural networks. *IEEE Transactions on Signal Processing* 45, 11 (1997), 2673–2681.
- [144] Sungyong Seo, Jing Huang, Hao Yang, and Yan Liu. 2017. Interpretable convolutional neural networks with dual local and global attention for review rating prediction. In *Proceedings of the Eleventh ACM Conference on Recommender Systems*. 297–305.
- [145] Yan Shi, Haoran Feng, Xiongfei Geng, Xingui Tang, and Yongcai Wang. 2019. A Survey of Hybrid Deep Learning Methods for Traffic Flow Prediction. In *Proceedings of the 2019 3rd International Conference on Advances in Image Processing*. Association for Computing Machinery, 133–138.
- [146] S. Shin, H. Jeon, C. Cho, S. Yoon, and T. Kim. 2020. User Mobility Synthesis based on Generative Adversarial Networks: A Survey. In *2020 22nd International Conference on Advanced Communication Technology (ICACT)*. 94–103.
- [147] Filippo Simini, Gianni Barlacchi, Massimiliano Luca, and Luca Pappalardo. 2020. Deep Gravity: enhancing mobility flows generation with deep neural networks and geographic information. arXiv:cs.LG/2012.00489
- [148] Filippo Simini, Marta C. González, Amos Maritan, and Albert-László Barabási. 2012. A universal model for mobility and migration patterns. *Nature* 484, 7392 (2012), 96–100.

- [149] Karen Simonyan and Andrew Zisserman. 2015. Very Deep Convolutional Networks for Large-Scale Image Recognition. In *Proceedings of the 3rd International Conference on Learning Representations*, Yoshua Bengio and Yann LeCun (Eds.).
- [150] SoBigData. 2015. *SoBigData catalogue*. <https://sobigdata.d4science.org/catalogue-sobigdata>
- [151] B. H. Soleimani, E. N. De Souza, C. Hilliard, and S. Matwin. 2015. Anomaly detection in maritime data based on geometrical analysis of trajectories. In *2015 18th International Conference on Information Fusion (Fusion)*. 1100–1105.
- [152] G. Solmaz and D. Turgut. 2019. A Survey of Human Mobility Models. *IEEE Access* 7 (2019), 125711–125731.
- [153] Chaoming Song, Tal Koren, Pu Wang, and Albert-László Barabási. 2010. Modelling the scaling properties of human mobility. *Nature Physics* 6, 10 (2010), 818–823.
- [154] Chaoming Song, Zehui Qu, Nicholas Blumm, and Albert-László Barabási. 2010. Limits of predictability in human mobility. *Science* 327, 5968 (2010), 1018–1021.
- [155] H. Y. Song, M. S. Baek, and M. Sung. 2019. Generating Human Mobility Route Based on Generative Adversarial Network. In *2019 Federated Conference on Computer Science and Information Systems (FedCSIS)*. 91–99.
- [156] Xuan Song, Quanshi Zhang, Yoshihide Sekimoto, Ryosuke Shibasaki, Nicholas Jing Yuan, and Xing Xie. 2016. Prediction and Simulation of Human Mobility Following Natural Disasters. *ACM Transactions on Intelligent Systems and Technologies* 8, 2 (2016).
- [157] Victor Soto, Vanessa Frias-Martinez, Jesus Virseda, and Enrique Frias-Martinez. 2011. Prediction of socioeconomic levels using cell phone records. In *International Conference on User Modeling, Adaptation, and Personalization*. 377–388.
- [158] University of Maryland Start. 2009. *Global Terrorism Database*. <http://www.start-dev.umd.edu/gtd/>
- [159] Iain D Stewart, Chris A Kennedy, Angelo Facchini, and Renata Mele. 2018. The electric city as a solution to sustainable urban development. *Journal of Urban Technology* 25, 1 (2018), 3–20.
- [160] Arkadiusz Stopczynski, Vedran Sekara, Piotr Sapiezynski, Andrea Cuttone, Mette My Madsen, Jakob Eg Larsen, and Sune Lehmann. 2014. Measuring Large-Scale Social Networks with High Resolution. *PLOS ONE* 9, 4 (2014), 1–24.
- [161] Junkai Sun, Junbo Zhang, Qiaofei Li, Xiuwen Yi, and Yu Zheng. 2019. Predicting citywide crowd flows in irregular regions using multi-view graph convolutional networks. *arXiv preprint arXiv:1903.07789* (2019).
- [162] Ilya Sutskever, Oriol Vinyals, and Quoc V Le. 2014. Sequence to sequence learning with neural networks. In *Advances in neural information processing systems*. 3104–3112.
- [163] Andrew J Tatem. 2014. Mapping the denominator: spatial demography in the measurement of progress. *International health* 6, 3 (2014), 153–155.
- [164] Andrew J Tatem. 2017. WorldPop, open data for spatial demography. *Scientific data* 4, 1 (2017), 1–4.
- [165] Bart Thomee, David A. Shamma, Gerald Friedland, Benjamin Elizalde, Karl Ni, Douglas Poland, Damian Borth, and Li-Jia Li. 2016. YFCC100M. *Commun. ACM* 59, 2 (2016), 64–73.
- [166] Chujie Tian, Xinning Zhu, Zheng Hu, and Jian Ma. 2020. Deep spatial-temporal networks for crowd flows prediction by dilated convolutions and region-shifting attention mechanism. *Applied Intelligence* (2020), 1–14.
- [167] New York City TLC. 2009. *New York City Taxi & Limousine Commission*. <https://www1.nyc.gov/site/tlc/about/tlc-trip-record-data.page>
- [168] Marcello Tomasini, Basim Mahmood, Franco Zambonelli, Angelo Brayner, and Ronaldo Menezes. 2017. On the effect of human mobility to the design of metropolitan mobile opportunistic networks of sensors. *Pervasive and Mobile Computing* 38 (2017), 215 – 232.
- [169] Jameson Toole, Carlos Herrera-Yague, Christian Schneider, and Marta C. Gonzalez. 2015. Coupling Human Mobility and Social Ties. *Journal of the Royal Society Interface* 12 (2015).
- [170] Alexander Toshev and Christian Szegedy. 2014. DeepPose: Human Pose Estimation via Deep Neural Networks. In *Proceedings of the 2014 IEEE Conference on Computer Vision and Pattern Recognition*. IEEE Computer Society, 1653–1660.
- [171] International Telecommunication Union. 2019. *Measuring digital development Facts and figures*. Technical Report. International Telecommunication Union.
- [172] Michele Vespe, Maurizio Gibin, Alfredo Alessandrini, Fabrizio Natale, Fabio Mazzarella, and Giacomo C. Osio. 2016. Mapping EU fishing activities using ship tracking data. *Journal of Maps* 12, sup1 (2016), 520–525.
- [173] Vasiliki Voukelatou, Lorenzo Gabrielli, Ioanna Miliou, Stefano Cresci, Rajesh Sharma, Maurizio Tesconi, and Luca Pappalardo. 2020. Measuring objective and subjective well-being: dimensions and data sources. *International Journal of Data Science and Analytics* (2020).
- [174] Di Wang, Tomio Miwa, and Takayuki Morikawa. 2020. Big Trajectory Data Mining: A Survey of Methods, Applications, and Services. *Sensors* 20, 16 (2020), 4571.
- [175] Jinzhong Wang, Xiangjie Kong, Feng Xia, and Lijun Sun. 2019. Urban human mobility: Data-driven modeling and prediction. *ACM SIGKDD Explorations Newsletter* (2019), 1–19.
- [176] Leye Wang, Xu Geng, Xiaojuan Ma, Feng Liu, and Qiang Yang. 2018. Cross-city transfer learning for deep spatio-temporal prediction. *arXiv preprint arXiv:1802.00386* (2018).
- [177] Yan Wang and John E Taylor. 2018. Coupling sentiment and human mobility in natural disasters: a Twitter-based study of the 2014 South Napa Earthquake. *Natural hazards* 92, 2 (2018), 907–925.
- [178] Billy M Williams and Lester A Hoel. 2003. Modeling and forecasting vehicular traffic flow as a seasonal ARIMA process: Theoretical basis and empirical results. *Journal of transportation engineering* 129, 6 (2003), 664–672.

- [179] Ruizhi Wu, Guangchun Luo, Junming Shao, L. Tian, and Chengzong Peng. 2018. Location prediction on trajectory data: A review. *Big Data Min. Anal.* 1 (2018), 108–127.
- [180] Peng Xie, Tianrui Li, Jia Liu, Shengdong Du, Xin Yang, and Junbo Zhang. 2020. Urban flow prediction from spatiotemporal data using machine learning: A survey. *Information Fusion* 59 (2020), 1–12.
- [181] SHI Xingjian, Zhouong Chen, Hao Wang, Dit-Yan Yeung, Wai-Kin Wong, and Wang-chun Woo. 2015. Convolutional LSTM network: A machine learning approach for precipitation nowcasting. In *Advances in neural information processing systems*. 802–810.
- [182] Kelvin Xu, Jimmy Ba, Ryan Kiros, Kyunghyun Cho, Aaron Courville, Ruslan Salakhudinov, Rich Zemel, and Yoshua Bengio. 2015. Show, attend and tell: Neural image caption generation with visual attention. In *International conference on machine learning*. 2048–2057.
- [183] Shuai Xu, Xiaoming Fu, Jiuxin Cao, Bo Liu, and Zhixiao Wang. 2020. Survey on user location prediction based on geo-social networking data. *World Wide Web* (2020), 1–44.
- [184] Zhaojin Yan, Yijia Xiao, Liang Cheng, Rong He, Xiaoguang Ruan, Xiao Zhou, Manchun Li, and Ran Bin. 2020. Exploring AIS data for intelligent maritime routes extraction. *Applied Ocean Research* 101 (2020), 102271.
- [185] Dingqi Yang, Benjamin Fankhauser, Paolo Rosso, and Philippe Cudre-Mauroux. 2020. Location Prediction over Sparse User Mobility Traces Using RNNs: Flashback in Hidden States!. In *Proceedings of the Twenty-Ninth International Joint Conference on Artificial Intelligence, IJCAI-20*. 2184–2190.
- [186] Dingqi Yang, Bingqing Qu, Jie Yang, and Philippe Cudre-Mauroux. 2019. Revisiting User Mobility and Social Relationships in LBSNs: A Hypergraph Embedding Approach. 2147–2157.
- [187] Dingqi Yang, Daqing Zhang, Longbiao Chen, and Bingqing Qu. 2015. NationTelescope: Monitoring and visualizing large-scale collective behavior in LBSNs. *Journal of Network and Computer Applications* 55 (2015), 170–180.
- [188] Dingqi Yang, Daqing Zhang, and Bingqing Qu. 2015. Participatory cultural mapping based on collective behavior in location based social networks. *ACM Transactions on Intelligent Systems and Technology* (2015). in press.
- [189] Dingqi Yang, Daqing Zhang, Bingqing Qu, and Philippe Cudre-Mauroux. 2016. PrivCheck: privacy-preserving check-in data publishing for personalized location based services. In *Proceedings of the 2016 ACM International Joint Conference on Pervasive and Ubiquitous Computing*. ACM, 545–556.
- [190] Dingqi Yang, Daqing Zhang, Vincent. W. Zheng, and Zhiyong Yu. 2015. Modeling User Activity Preference by Leveraging User Spatial Temporal Characteristics in LBSNs. *IEEE Transactions on Systems, Man, and Cybernetics: Systems* 45, 1 (2015), 129–142.
- [191] Di Yao, Chao Zhang, Jianhui Huang, and Jingping Bi. 2017. Serm: A recurrent model for next location prediction in semantic trajectories. In *Proceedings of the 2017 ACM on Conference on Information and Knowledge Management*. 2411–2414.
- [192] Huaxiu Yao, Xianfeng Tang, Hua Wei, Guanjie Zheng, and Zhenhui Li. 2019. Revisiting Spatial-Temporal Similarity: A Deep Learning Framework for Traffic Prediction. In *2019 AAAI Conference on Artificial Intelligence (AAAI'19)*.
- [193] Yelp. 2017. *Yelp Open Dataset*. <https://www.yelp.com/dataset>
- [194] Dan Yin and Qing Yang. 2018. GANs based density distribution privacy-preservation on mobility data. *Security and Communication Networks* 2018 (2018).
- [195] Xueyan Yin, Genze Wu, Jinze Wei, Yanming Shen, Heng Qi, and Bao cai Yin. 2020. A Comprehensive Survey on Traffic Prediction. *arXiv preprint arXiv:2004.08555* (2020).
- [196] Lantao Yu, Weinan Zhang, Jun Wang, and Yong Yu. 2017. Seqgan: Sequence generative adversarial nets with policy gradient. In *Thirty-first AAAI conference on artificial intelligence*.
- [197] Hao Yuan, Xinning Zhu, Zheng Hu, and Chunhong Zhang. 2020. Deep Multi-View Residual Attention Network for Crowd Flows Prediction. *Neurocomputing* (2020).
- [198] Chao Zhang, Jiawei Han, Lidan Shou, Jiajun Lu, and Thomas LLa Porta. 2014. Splitter: Mining fine-grained sequential patterns in semantic trajectories. *Proceedings of the VLDB Endowment* 7, 9 (2014), 769–780.
- [199] Chao Zhang, Keyang Zhang, Quan Yuan, Luming Zhang, Tim Hanratty, and Jiawei Han. 2016. Gmove: Group-level mobility modeling using geo-tagged social media. In *Proceedings of the 22nd ACM SIGKDD International Conference on Knowledge Discovery and Data Mining*. 1305–1314.
- [200] G Peter Zhang. 2003. Time series forecasting using a hybrid ARIMA and neural network model. *Neurocomputing* 50 (2003), 159–175.
- [201] Junbo Zhang, Yu Zheng, and Dekang Qi. 2017. Deep spatio-temporal residual networks for citywide crowd flows prediction. In *Thirty-First AAAI Conference on Artificial Intelligence*.
- [202] K. Zhao, S. Tarkoma, S. Liu, and H. Vo. 2016. Urban human mobility data mining: An overview. In *2016 IEEE International Conference on Big Data (Big Data)*. 1911–1920.
- [203] Liang Zhao. 2020. Event Prediction in Big Data Era: A Systematic Survey. *arXiv preprint arXiv:2007.09815* (2020).
- [204] Xin Zheng, Jialong Han, and Aixin Sun. 2018. A survey of location prediction on twitter. *IEEE Transactions on Knowledge and Data Engineering* 30, 9 (2018), 1652–1671.
- [205] Yu Zheng. 2011. T-Drive trajectory data sample.
- [206] Yu Zheng. 2015. Trajectory data mining: an overview. *ACM Transactions on Intelligent Systems and Technology (TIST)* (2015), 1–41.

- [207] Yu Zheng, Licia Capra, Ouri Wolfson, and Hai Yang. 2014. Urban computing: concepts, methodologies, and applications. *ACM Transactions on Intelligent Systems and Technology (TIST)* 5, 3 (2014), 1–55.
- [208] Yu Zheng, Xing Xie, Wei-Ying Ma, et al. 2010. GeoLife: A collaborative social networking service among user, location and trajectory. *IEEE Data Eng. Bull.* 33, 2 (2010), 32–39.
- [209] Yirong Zhou, Ye Wu, Jiangjiang Wu, Luo Chen, and Jun Li. 2018. Refined Taxi Demand Prediction with ST-Vec. In *2018 26th International Conference on Geoinformatics*. IEEE, 1–6.
- [210] Wen-Yuan Zhu, Wen-Chih Peng, Ling-Jyh Chen, Kai Zheng, and Xiaofang Zhou. 2015. Modeling User Mobility for Location Promotion in Location-Based Social Networks. In *Proceedings of the 21th ACM SIGKDD International Conference on Knowledge Discovery and Data Mining*. 1573–1582.
- [211] Ali Zonoozi, Jung-jae Kim, Xiao-Li Li, and Gao Cong. 2018. Periodic-CRN: A Convolutional Recurrent Model for Crowd Density Prediction with Recurring Periodic Patterns.. In *IJCAI*. 3732–3738.